



Skolkovo Institute of Science and Technology

MASTER'S THESIS

Topological Josephson Tunnel junctions

Master's Educational Program: Theoretical and mathematical physics

Student_____

Anton Naumov

Theoretical and mathematical physics

May 31, 2019

Research Advisor:_____

Pavel Ioselevich

Associate Professor

Co-Advisor:_____

Mikhail Skvortsov

Associate Professor

Moscow 2019

All rights reserved.©

The author hereby grants to Skoltech permission to reproduce and to distribute publicly paper and electronic copies of this thesis document in whole and in part in any medium now known or hereafter created.

Topological Josephson Tunnel junctions

Anton Naumov

Submitted to the Skolkovo Institute of Science and Technology
on May 31, 2019

Abstract

Topological superconductivity is relatively fresh topic of condensed matter physics. Being a rich platform for intriguing and beautiful problems, it also has a huge and unrevealed potential for technology, especially for quantum computing.

The notion of topological superconductivity is closely related to a possibility of presence of a Majorana state — special topologically protected state, usually localized near some inhomogeneity in a topological superconductor. Despite the numerous theoretical proposals of construction this state in condensed matter, its observation in experimental setup is still big challenge

In this work the system of two one-dimensional superconducting wires connected with a tunnel junction is considered. Under special conditions this system can host a Majorana fermion. The properties of this system, such as subgap states, stationary supercurrent and ionization under oscillating external voltage are studied. The results of this work have the potential in developing a new technique of detecting Majorana fermions in such systems.

Research Advisor:

Name: Pavel Ioselevich

Degree: PhD in Theoretical physics, Doctor of science

Title: Associate Professor

Co-Advisor:

Name: Mikhail Skvortsov

Degree: Professor,

Title: Associate Professor

Contents

1	Introduction	5
2	The model	6
2.1	Problem statement	6
2.2	The dispersion of a homogeneous wire	8
2.3	High and low modes	10
3	Stationary properties	11
3.1	Boundary condition	11
3.2	High momentum modes	12
3.3	Eliminating longwave modes from boundary condition	13
3.4	Low momenta and linearized Hamiltonian	15
3.5	Subgap states	17
3.5.1	The case of zero tunneling	18
3.5.2	Small tunneling	19
3.6	Stationary supercurrent	20
3.6.1	E between $ g_L $ and g_R	22
3.6.2	E is greater than both $ g_L $ and g_R and much smaller than Δ	22
3.6.3	E is near and below Δ	23
3.6.4	Analysing the results	24
4	Ionization	25
4.1	Introducing the perturbation	25
4.2	Tunnel Hamiltonian approach	26
4.3	Ionization rate for $g_R \gg g_L $	28
4.3.1	Time dependence of perturbation	28
4.3.2	Factorizing $w_{\mathcal{E}}$	29
4.3.3	Using multinomial formula	30
4.3.4	Pure Andreev regime	31
4.3.5	Andreev+Normal regime	35
4.4	Results	38

5	Discussion	40
5.0.1	Results summary	40
5.0.2	Possible experimental realization	40
6	Conclusion	42
A	Wavefunctions for the stationary contact	43
B	Multiphoton ionization	46
B.1	Basics about Green's functions	46
B.2	Fermi Golden Rule (first order)	47
B.3	Fermi Golden Rule (high order)	49

Chapter 1

Introduction

The system, considered in this work, is a pair of 1D superconductors connected with a Josephson junction. For all the discussion presented it's crucial for one of superconductors to be topological.

Topological superconductivity is relatively fresh topic in physics. On the one hand it's being connected to particle physics through the notion of Majorana fermion – the particle coinciding with it's own antiparticle[1]. It can be looked for not only in Standart models' context[2][3][4], but also as a state in solids[5][6][7][8][9][10][11][12][13][14][15][16]. Despite the difference between these entities, there is a clear analogy between majoranas in condensed matter and majoranas in particle physics[17][18].

On the other hand topological superconductivity is of interest to quantum computation community as a platform to build fault tolerant quantum memory[6][19][20][21]. Although significant difficulties has appeared on this way, the intention to realize this program is still strong and gives the motivation to build a superconducting samples, which demonstrates signatures of nontrivial topology and presence of Majorana fermions[22][23][24].

The proposition of using superconducting wires as a carriers of Majorana fermions came from a seminal work of Kitaev [6]. The key ingredient of this system was a p-wave superconductivity assumed to be present in a wire. There was showed, that under certain conditions the Majroana state ca be present at the end of the wire. After some time another propositions[25][26] appeared, based on semiconductor-superconductor heterostructures with s-wave superconductivity, external magnetic field and spin-orbit coupling. It was showed, that the sign of quantity $g = B = \sqrt{B^2 + \mu^2}$, where B is a magnetic field, Δ is the absolute value of superconducting order parameter and μ is a chemical potential can be used as a topological index, and a Majorana state will appear where $\text{sgn } g$ is changing.

The model, considered is this work is close to the ones used in [25][26]. It consists of two superconducting wires connected with a tunnel junction. However instead of domain wall of $\text{sgn } g$, a tunnel barrier between areas with $g > 0$ and $g < 0$ is introduced. This model formulated in detail in chapter 2. The spectrum of this model and stationary supercurrent are studied in chapter 3 and the ionization under small external oscillating voltage is considered in chapter 4. Chapter 5 stands for the discussion of obtained results and their possible experimental realization and use, while chapter 6 to conclusion chapter concludes the study.

Chapter 2

The model

The model studied here is mostly inspired by the works [25] and [26]. Here, however, some more complications are present to make it better reflecting possible experimental situation and catch some higher energy effects that in [25] and [26].

2.1 Problem statement

The system under consideration consists of two 1D s-wave superconducting wires connected with a tunnel junction. There is a strong spin-orbit coupling assumed to be present and external magnetic field is applied in the direction perpendicular to the wire. The Hamiltonian of the bulk of each wire, written in the Bogoliubov-de Gennes formalism, is similar to the ones presented in [25] and [26]:

$$\mathcal{H} = \int dy \Psi^\dagger(y) H \Psi(y) \quad \Psi = \begin{pmatrix} \psi_\uparrow \\ \psi_\downarrow \\ \psi_\downarrow^\dagger \\ -\psi_\uparrow^\dagger \end{pmatrix} \quad (2.1)$$

$$H = \left(\frac{p^2}{2m} - \mu_0 \right) \tau_z + up\sigma_z\tau_z + B\sigma_x + \Delta\tau_\phi \quad (2.2)$$

Here σ_i and τ_i are Pauli matrices in spin and particle-hole subspaces respectively, $\tau_\phi = \tau_x \cos \phi - \tau_y \sin \phi$, with ϕ being a superconducting phase, μ_0 is a chemical potential, B is an external magnetic field, Δ is the absolute value of superconducting order parameter and u is spin-orbit coupling constant with the dimension of velocity. The wire is being aligned along the y-axis, while the direction of the magnetic field coincides with x-axis. Note, that only one component of spin-orbit is nonzero due to 1D nature of the problem.

The tunnel junction is introduced by applying an external electrical field. Its potential profile $U(y)$ is presented on figure 2.1(a). Inside each wire the potential is assumed to be homogeneous, though its value can be different to the right and to the left of the junction. The junction itself is modeled by a sharp peak of the potential.

To take this into account one should include an additional term $U(y)\tau_z$ in (2.2). However this term can be combined with the second term of by (2.2) by introducing an effective chemical

potential $\mu(y) = \mu_0 - U(y)$ (see figure 2.1(b)). From now on all presence of the external field will be hidden in $\mu(y)$.

The superconducting phase ϕ in left and right wires, ϕ_L and ϕ_R , can also be different. The phase inside the barrier is undefined as $\Delta(y) = 0$ there.

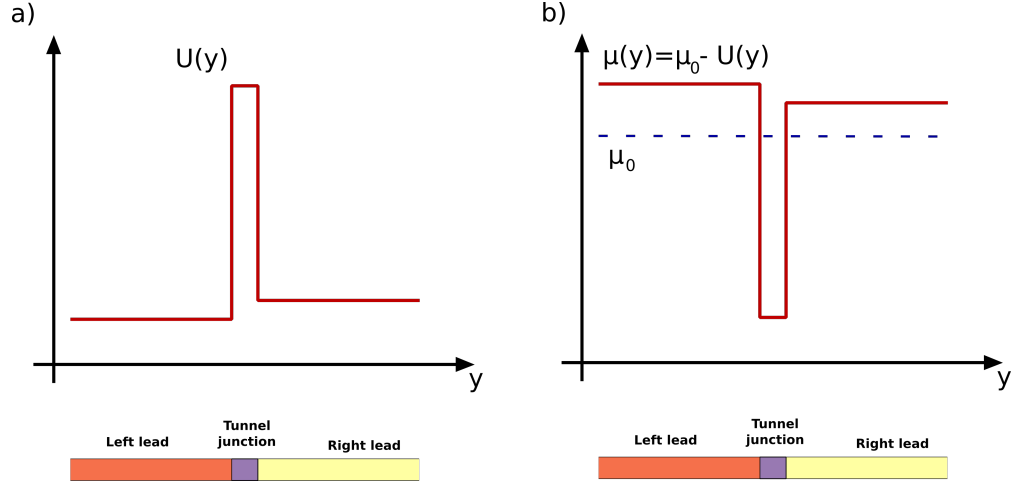


Figure 2.1: (a) y -profile of external electrical field. (b) y -profile of effective chemical potential

Finally, the BdG Hamiltonian for the model reads:

$$H = \left(\frac{p^2}{2m} - \mu(y) \right) \tau_z + up\sigma_z\tau_z + B\sigma_x + \Delta(y) \tau_{\phi(y)} \quad (2.3)$$

with

$$\mu(y) = \begin{cases} \mu_L, & -\frac{L}{2} < y \\ \mu_b, & -\frac{L}{2} < y < \frac{L}{2} \\ \mu_R, & \frac{L}{2} < y \end{cases} \quad \Delta(y) = \begin{cases} \Delta, & y > \frac{L}{2}, y < -\frac{L}{2} \\ 0, & -\frac{L}{2} < y < \frac{L}{2} \end{cases} \quad (2.4)$$

$$\phi(y) = \begin{cases} \phi_L, & -\frac{L}{2} < y \\ \phi_R, & \frac{L}{2} < y \end{cases} \quad (2.5)$$

with L being the size of the junction. Note, that the parameters B , u , Δ and m are taken to be constant across the system.

This setup is close to one of the models considered by Oreg et al. in [25] (*"Spatially varying μ "* section). The difference is in the profile of $\mu(y)$ – in [25] there is a step in effective chemical potential, while here this function possesses a well.

In [25] it's also discussed that the Majorana fermion appears at the inhomogeneity if the difference $B - \sqrt{\mu^2 + \Delta^2}$ is greater than zero on one side of the step in $\mu(y)$ and lesser than zero on another side of it. As will be shown further, this is also relevant to the system presented here.

Note, that if $B > |\Delta|$ this condition can always be satisfied by choosing appropriate μ_L and μ_R .

When the two wires of different sign of g are assumed in this work, the trivial wire will always be on the left, while the topological wire will always be on the right.

The model, described by (2.3) and (2.4) possesses a big number of external parameters. Different areas in this parameter space require different approaches and sometimes lead to completely different physics. Here the certain experimentally reasonable constraints are assumed:

$$\mu_L, \mu_R \ll B \sim \Delta \ll mu^2 \ll |\mu_b| \quad (2.6)$$

The experimental justification of this choice is given in the chapter 5, while call for it from theoretical point of view will arise further in this chapter.

2.2 The dispersion of a homogeneous wire

Before discussing the properties of the junction it's necessary to consider a dispersion of a homogeneous wire modeled with the Hamiltonian (2.2). Although this can be done exactly, it's instructive to obtain this dependence step by step, starting with a simpler model and adding new terms until the Hamiltonian (2.2) is restored.

The starting point is the Hamiltonian consisting only of kinetic energy and chemical potential terms: $H = \frac{p^2}{2m} - \mu$. It has simple parabolic dispersion presented at fig. 2.2(a). When the spin is introduced and spin-orbit coupling term $up\sigma_z$ is added, the parabola splits in two (fig. 2.2(b)), each one corresponding to it's own z-protection of the spin. After introducing a magnetic field with $B\sigma_x$ term, the gap at the intersection opens (fig. 2.2(c)). The next step is introducing the BdG formalism, by adding the multiplier τ_z elsewhere except for magnetic field term: $H = \left(\frac{p^2}{2m} - \mu_0\right)\tau_z + up\sigma_z\tau_z + B\sigma_x$. This procedure doubles the spectra in a way that each eigenvector with energy E obtains a partner eigenvector with energy $-E$, so additional two energy branches appear, being a mirror reflection of initial dispersion. This is presented at fig. 2.2(d), with the dashed lines being BdG partners. The last step is adding the superconducting term $\Delta\tau_\phi$, which opens the gap where the dashed and the solid lines are intersected (fig. 2.2(e)).

As was mentioned before, the dispersion can be found explicitly. As was pointed in [25], it can be done by squiring the Hamiltonian (2.2) twice and solving a resulting biquadratic equation, leading to:

$$E_{1,2}^2(p) = B^2 + \Delta^2 + \xi_p^2 + (up)^2 \pm 2\sqrt{B^2\Delta^2 + B^2\xi_p^2 + (up)^2\xi_p^2} \quad (2.7)$$

with $\xi_p = \frac{p^2}{2m} - \mu$. This dependence, presented at fig. 2.2(f), has two positive and two negative branches, as any BdG dispersion with electron-hole symmetry does. It further discussion only positive branches are considered, if opposite is not mentioned.

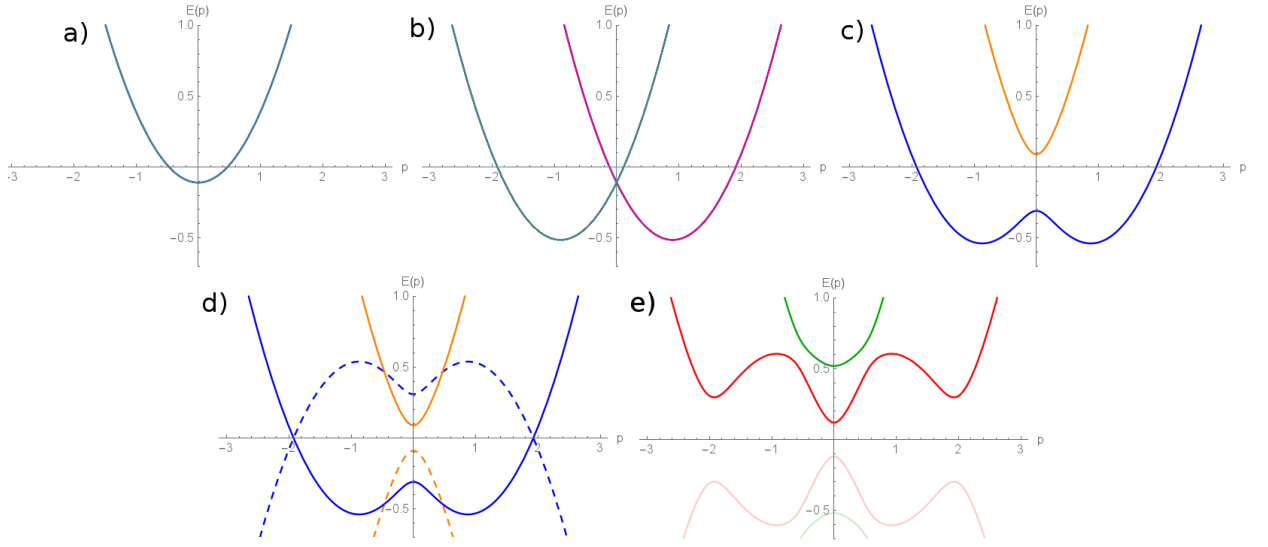


Figure 2.2: The dispersion of different Hamiltonians: a) mere kinetic energy and chemical potential: $H = \frac{p^2}{2m} - \mu$ b) spin-orbit coupling added: $H = \frac{p^2}{2m} - \mu_0 + up\sigma_z$ c) magnetic field added: $H = \frac{p^2}{2m} - \mu_0 + up\sigma_z + B\sigma_x$ d) BdG formalism introduced: $H = \left(\frac{p^2}{2m} - \mu_0\right)\tau_z + up\sigma_z\tau_z + B\sigma_x$ e) The complete Hamiltonian of homogeneous wire: $H = \left(\frac{p^2}{2m} - \mu_0\right)\tau_z + up\sigma_z\tau_z + B\sigma_x + \Delta\tau_\phi$. The parameters of the Hamiltonians for the plotting are: $B = 0.2$, $\Delta = 0.3$, $u = 0.9$, $m = 1$, $\mu = 0.11$

If the constrains (2.6) are assumed, the lower branch of this spectra has three minima: one of them is at $p = 0$ exactly, and two another are at $p = \pm 2mu$ in the leading order. The last two are not very interesting – the energy there is approximately equal to Δ , as it should be due to perturbative introduction of superconducting term. On the contrary, the minimum at $p = 0$, which is given by[25]:

$$E_2(0) = |g|, \quad g = B - \sqrt{\Delta^2 + \mu^2} \quad (2.8)$$

is the most important peculiarity of the spectrum. First, as $\mu \ll B \sim \Delta$, it's the true gap of the spectrum as $\left|B^2 - \sqrt{\Delta^2 + \mu^2}\right| \approx \left|B - \Delta - \frac{\mu^2}{2\Delta}\right| \ll \Delta$. Second, the sign of g defines where the wire can or cannot host the Majorana state near some inhomogeneity. Here it's useful to introduce the terminology: if $g > 0$ the wire is called "topological", otherwise it's called "trivial". In [25] and [26] it was derived, that the contact of trivial and topological wire hosts a Majorana state. It can also be shown (see section 3.5.1), that this state is present on the end of a topological wire and isn't there for a trivial one.

Note, that when two wires are considered, there are two gaps, $g_{L,R} = B - \sqrt{\Delta^2 + \mu_{L,R}^2}$. When the magnetic field B is close to Δ , one can change the signs of $g_{L,R}$ by changing $\mu_{L,R}$ respectively.

It's instructive to clarify the place of $g_{L,R}$ in the parameter hierarchy of the problem. As

$\mu_L \sim \mu_R \ll B \sim \Delta$ and $g_L = B - \sqrt{\Delta^2 + \mu_L^2} < 0$, one can figure out that $\mu_R \sim \mu_L \gtrsim (B - \Delta)(B + \Delta)$. Taking that into account and noticing that $g_{L,R} \approx B - \Delta - \frac{\mu^2}{2\Delta^2}$ and introducing $\beta = B - \Delta$ one finds $g_{L,R} \lesssim \frac{\beta^2}{\Delta}$, while $\mu_{L,R} \gtrsim \sqrt{\beta\Delta}$, so $\sqrt{\beta} \ll \mu_L, \mu_R$.

2.3 High and low modes

Though the wavefunctions of (2.2) can be found explicitly, their form is enough complicated to stall any further analysis. However, as the spin-orbit energy is assumed to be the biggest energy scale for a homogeneous wire, one can reduce the Hamiltonian (2.2) to:

$$H = \left(\frac{p^2}{2m} + up\sigma_z \right) \tau_z \quad (2.9)$$

in this problem it's reasonable to assume the low energy limit, as all the Majorana physics should live at the energies of the order of g . Thus the energy term must be omitted in Schroedinger equation, which leads to two types of momenta: $p_{short} \approx \pm 2mu$ and $p_{long} \approx 0$ and, respectively two types of wavefunctions: shortwave and longwave ones. The fact that p_{long} is equal to zero means, that the approximation (2.9) is insufficient to describe them. However, to deal with long-wave wavefunctions one can omit the quadratic term in (2.2) and work with linearized Hamiltonian, similar to the ones used in [25] and [26].

Chapter 3

Stationary properties

The stationary properties of the system are defined by it's spectrum. In this chapter the boundary condition is introduced, wavefunctions of the homogeneous wires are obtained, undergap states are investigated and the stationary supercurrent is estimated.

3.1 Boundary condition

To obtain the spectrum of the system it's necessary to find the boundary conditions. As the barrier chemical potential is the biggest energy parameter of the problem, the wave-functions there are defined by the Hamiltonian:

$$H(y) = \left(\frac{p^2}{2m} + \mu_b \right) \tau_z, \quad -\frac{L}{2} < y < \frac{L}{2} \quad (3.1)$$

as the low energies are the under consideration, in Sroedinger equation the energy term can be omitted, so $p_b \approx \pm i\sqrt{2m\mu_b}$. One can solve the problem given by (3.1) and match the values of the wavefunction and it's derivatives on the left and on the right of the barrier to obtain:

$$\begin{cases} \psi_L + b\partial_y\psi_L = t(\psi_R + b\partial_y\psi_R) \\ \psi_R - b\partial_y\psi_R = t(\psi_L - b\partial_y\psi_L) \end{cases} \quad (3.2)$$

here $\psi_{L,R} = \psi(\mp \frac{L}{2})$, $b = (2m\mu_b)^{-\frac{1}{2}}$ — the penetration depth for the particle inside the barrier and $t = e^{-\frac{L}{b}}$ — the tunneling constant assumed to be small: $t \ll 1$. This condition reads, that the size of the barrier L should be much bigger than the penetration depth b .

This condition is invariant under the combined action $L \leftrightarrow R$, $y \rightarrow -y$. To simplify the further analysis one can reverse the direction in the left wire and put both ends of the wires from $y = \frac{L}{2}$ to $y = 0$. The boundary condition then becomes:

$$\begin{cases} \psi_L - b\partial_y\psi_L = t(\psi_R + b\partial_y\psi_R) \\ \psi_R - b\partial_y\psi_R = t(\psi_L + b\partial_y\psi_L) \end{cases} \quad (3.3)$$

This transformation is illustrated on the fig 3.1. Note

The boundary condition (3.3) can be rewritten with introducing the spinor $\Psi = (\psi_L, \psi_R)^T$ and Pauli matrices \hat{s}_i in LR space:

$$(1 - t\hat{s}_x) \Psi - (1 + t\hat{s}_x) b\partial_y \Psi = 0 \quad (3.4)$$

since for all $t \neq 1$ (recall, that $t \ll 1$) the matrix is $1 \pm t\hat{s}_x$ in reversible. Multiplying the last equation by $(1 - t\hat{s}_x) / (1 + t^2)$ one obtain:

$$\left(1 - 2\tilde{t}\hat{s}_z - \tilde{b}\partial_y\right) \psi = 0 \quad (3.5)$$

where $\tilde{t} = \frac{t}{1+t^2}$, $\tilde{b} = \frac{1-t^2}{1+t^2}b$. In the leading order on t , which corresponds to the tunneling limit, $\tilde{t} = t$, $\tilde{b} = b$.

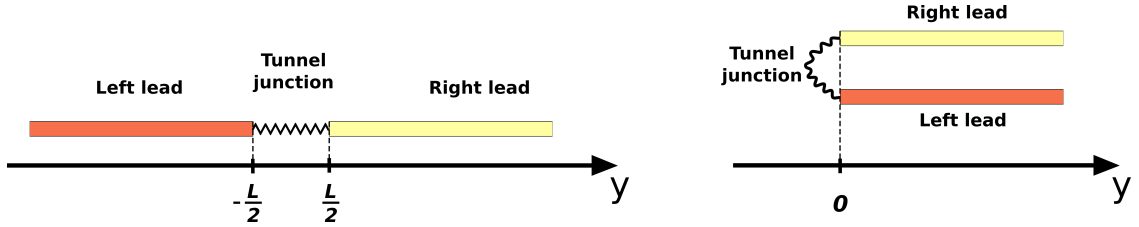


Figure 3.1: Illustration of switching the direction of left wire

One can argue, that in tunneling limit the second and the third term in (3.5) are much smaller than the first one and should not be taken when the leading order is considered. However, if the second terms is omitted, the leads become efficiently disconnected, and no tunnel effects can be found. The same is true for the third term — if it's not present, the boundary condition immediately implies $\Psi(0) = 0$, so the wires become disconnected again.

3.2 High momentum modes

As was pointed in section 2.3, there are two shortwave and longwave wavefunctions inside the wire, and the first ones can be described with the Hamiltonian (2.9). However, if one is looking for the localized states, even the longwave modes should be taken decaying. To obtain this, one needs to add a restore superconducting term in (2.9), so the spectrum become gapped and the momenta can get an imaginary part. So, for shortwave modes one should consider a Hamiltonian:

$$H = \left(\frac{p^2}{2m} - up\hat{s}_z\sigma_z \right) \tau_z + \Delta\tau_\phi \quad (3.6)$$

here the multiplier \hat{s}_z is added in the spin-orbit coupling term, as the direction of the left wire is inverted, so to write a correct Hamiltonian for LR space, one needs to change p to $-p$ for the left wire — which is exactly adding $-s_z$ multiplier to each momentum.

Denoting $\eta = \frac{p^2}{2m} - up\hat{s}_z\sigma_z$, one can rewrite (3.6) as $H = \eta\tau_z + \Delta\tau_\phi$. As $\hat{s}_z\sigma_z$ commutes with H one can treat it as a number, so the dispersion is $E^2 = \eta^2 + \Delta^2$ (the number corresponding to eigenstate of \hat{s}_z will be denoted as s_z while the number, corresponding to the eigenstate of σ_z will be denoted as ς_z). Thus $\eta = \pm i\sqrt{\Delta^2 - E^2}$, as the case $|E| < \Delta$ is assumed. For momenta one can write the equation:

$$p^2 - 2mus_z\varsigma_z p - 2m\eta = 0 \quad (3.7)$$

which for shortwave momenta gives $p_{short} \approx 2mus_z\varsigma_z + \frac{\eta}{u}s_z\varsigma_z$. Choosing the sign of η in a way, that the wavefunction decays at $x \rightarrow \infty$, one can obtain:

$$p_{short} \approx 2mus_z\varsigma_z + i\frac{\sqrt{\Delta^2 - E^2}}{u} \quad (3.8)$$

Now the wavefunction can be constructed by putting (3.8) into the Schroedinger equation $(\eta\tau_z + \Delta\tau_\phi)\Psi = E\Psi$. The solutions are:

$$\Psi_{s_z, \varsigma_z}(x) = \begin{pmatrix} 1 \\ e^{i(s_z\varsigma_z\gamma + \phi_{s_z})} \end{pmatrix}_{eh} e^{2imus_z\varsigma_z x - \frac{\sqrt{\Delta^2 - E^2}}{u}x} |s_z, \varsigma_z\rangle \quad (3.9)$$

where $|s_z, \sigma_z\rangle$ are eigenvectors of matrix $\hat{s}_z\sigma_z$, $\gamma = -\frac{\pi}{2} + \arcsin \frac{E}{\Delta}$ and $\phi_1 = \phi_L$, $\phi_{-1} = -\phi_R$. Thus the longwave part of eqigenstate can be written as:

$$\Psi_{long} = \sum_{s_z=\pm 1} \sum_{\varsigma_z=\pm 1} C_{s_z, \varsigma_z} \Psi_{s_z, \varsigma_z}(x) \quad (3.10)$$

3.3 Eliminating longwave modes from boundary condition

As the Majorana mode acts at low energies, it's expected to be predominantly longwave. This argument is in accord with [25] and [26], where the majorana state was an eigenstate of a linearized Hamiltonian, which is relevant only for longwave physics. So, it's reasonable to eliminate the shortwave modes from the problem, reformulating the boundary condition (2.9).

The wave function can be decomposed in shortwave and longwave parts: $\Psi = \Psi_{high} + \Psi_{low}$. inserting it into the(2.9) and using the fact, that $p_{low} \ll p_{high} \approx 2mus_z\sigma_z$, one can obtain at the

boundary:

$$(1 - 2t\hat{s}_x) \Psi_{low} + (1 - 2t\hat{s}_x - 2ibum\hat{s}_z\sigma_z) \Psi_{high} = 0 \quad (3.11)$$

Multiplying by the $(1 - 2t\hat{s}_x)^{-1}$ and eliminating t^2 terms, obtain:

$$\Psi_{low} = (-1 + i\zeta (1 + 2t\hat{s}_x) s_z \sigma_z) \Psi_{high} \quad (3.12)$$

with $\zeta = 2bum$.

Now, using the expansion (3.10) and renormalizing the coefficients: $C_{s_z\varsigma_z} \rightarrow -(1 - i\zeta s_z\varsigma_z) C_{s_z\varsigma_z}$ one can rewrite the boundary condition for ς_z spin component of the wavefunction as:

$$\Psi_{low,\varsigma_z} = \left(1 + \frac{2i\zeta t\hat{s}_z\sigma_z}{1 + i\zeta\hat{s}_z\sigma_z}\right) \sum_{s_z=\pm 1} C_{s_z,\varsigma_z} \begin{pmatrix} 1 \\ e^{i(s_z\varsigma_z\gamma+\phi_{s_z})} \end{pmatrix}_{eh} e^{2imus_z\varsigma_z x - \frac{\sqrt{\Delta^2 - E^2}}{u} x} |s_z, \varsigma_z\rangle \quad (3.13)$$

This can be multiplied by $\left(1 + \frac{2i\zeta t\hat{s}_z\sigma_z}{1 + i\zeta\hat{s}_z\sigma_z}\right)^{-1}$, which up to a t^2 correction yields:

$$\left(1 - \frac{2i\zeta t\hat{s}_z\sigma_z}{1 + i\zeta\hat{s}_z\sigma_z}\right) \Psi_{low,\varsigma_z} = \sum_{s_z=\pm 1} C_{s_z,\varsigma_z} \begin{pmatrix} 1 \\ e^{i(s_z\varsigma_z\gamma+\phi_{s_z})} \end{pmatrix}_{eh} e^{2imus_z\varsigma_z x - \frac{\sqrt{\Delta^2 - E^2}}{u} x} |s_z, \varsigma_z\rangle \quad (3.14)$$

For each ς_z the above equation can be interpreted as the requirement that the l.h.s. 4-vector (in LR- and eh-spaces) lies in the 2d linear space L_2 spanned by the two vectors in the sum in the r.h.s.. This can be reformulated as the requirement that the l.h.s. be orthogonal to the complementary 2d space \bar{L}_2 . There are two basic vectors $\bar{\Psi}_{s_z\varsigma_z}$ ($s_z = \pm 1$) spanning \bar{L}_2 for each ς_z :

$$\bar{\Psi}_{s_z\varsigma_z} = \begin{pmatrix} 1 \\ -e^{i(s_z\varsigma_z\gamma+\phi_{s_z})} \end{pmatrix} |s_z, \varsigma_z\rangle \quad (3.15)$$

Thus one needs to multiply (3.14) by $(\bar{\Psi}_{+\varsigma_z}, \bar{\Psi}_{-\varsigma_z})$ from the left and, after all evaluating the matrix product, find the boundary condition on longwave modes in the form:

$$\begin{pmatrix} 1 & -e^{-i(\varsigma_z\gamma-\phi_L)} & A & -Ae^{-i(\varsigma_z\gamma-\phi_L)} \\ A^* & -A^*e^{i(\varsigma_z\gamma+\phi_R)} & 1 & -e^{i(\varsigma_z\gamma+\phi_R)} \end{pmatrix} \Psi_{long,\varsigma_z} = 0 \quad (3.16)$$

here $A = -\frac{2i\zeta t\varsigma_z}{1+i\zeta\varsigma_z}$ and the elements are ordered as (Le, Lh, Re, Rh) .

When studying wavefunctions in superconductors, it is more convenient to work with zero phase ϕ . This can be achieved by gauging the phase difference into the boundary condition. In-

deed, suppose H_ϕ describes a wire with phase ϕ . Then, $H_\phi = U_\phi^\dagger H_0 U_\phi$ with $U_\phi = \text{diag}(1, e^{i\phi})_{eh}$ and the wave functions are also related via unitary rotation $\psi_\phi = U_\phi^\dagger \tilde{\psi}$. So the transform $U^\dagger = \text{diag}(1, e^{-i\phi_L}, 1, e^{-i\phi_R})_{Le,Lh,Re,Rh}$ will eliminate all the phases from the wires and put them into boundary condition. Substituting $\Psi_{low,\varsigma z} = U^\dagger \tilde{\Psi}$ into (3.16) one arrives at an even simpler boundary condition on the zero-phase function $\tilde{\Psi}$:

$$\begin{pmatrix} 1 & -e^{-i\varsigma z \gamma} & A & -Ae^{-i(\varsigma z \gamma + \varphi)} \\ A^* & -A^* e^{i(\varsigma z \gamma + \varphi)} & 1 & -e^{i\varsigma z \gamma} \end{pmatrix} \tilde{\Psi}_{long,\varsigma z} = 0 \quad (3.17)$$

where $\varphi = \phi_R - \phi_L$. Note, that any physical quantity can depend only on phase difference φ , but not on ϕ_L or ϕ_R separately.

It's also convenient to rewrite it in the form acting on the left and right wire wavefunctions:

$$M_L \tilde{\psi}_{low}^L + M_R \tilde{\psi}_{low}^R = 0$$

$$M_L = \begin{pmatrix} 1 & -e^{-i\sigma_z \gamma} \\ A^* & -A^* e^{i(\sigma_z \gamma + \varphi)} \end{pmatrix}_{eh} \quad M_R = \begin{pmatrix} A & -Ae^{i(\sigma_z \gamma + \varphi)} \\ 1 & -e^{i\sigma_z \gamma} \end{pmatrix}_{eh} \quad (3.18)$$

This for is especially useful for finding subgap states localized near the barrier.

3.4 Low momenta and linearized Hamiltonian

To utilize boundary condition (3.16) or (3.17), it's necessary to find low momenta wavefunctions in homogenous wire (this functions constitute ψ_{low} in (3.16) and (3.17). For this purpose one can use a linearized version of the Hamiltonian (2.2), like in [25] and [26]:

$$H = -\mu\tau_z + up\sigma_z\tau_z + B\sigma_x + \Delta\tau_x \quad (3.19)$$

here the zero phase ϕ is assumed and μ can be equal μ_L or μ_R depending on the wire considered. As was mentioned before, the nonzero phase can be restored by using U_ϕ matrix. This hamiltonian is valid only for the right wire. To obtain the solution in the left wire one needs to reverse the sign of p in (2.2). Instead of doing so, the unitary transform $\psi_L = \sigma_x \psi_R$ can be utilized, as for (2.2) $H(-p) = \sigma_x H(p) \sigma_x$.

Remembering, that $\beta = B - \Delta \ll B, \Delta$, one can treat this Hamiltonian penetratively,

decomposing it as $H = H_0 + V_0$:

$$H_0 = up\sigma_z\tau_z + \Delta(\sigma_x + \tau_x) \quad (3.20)$$

$$V = -\mu\tau_z + \beta\sigma_x \quad (3.21)$$

As H_0 commutes with $\sigma_x\tau_x$, it's convenient to rewrite it in the basis of common eigenstates of σ_x and τ_x . Denoting them as $|\sigma_x, \tau_x\rangle$ and arranging the order as $(|+, +\rangle, |-, -\rangle, |+, -\rangle, |-, +\rangle)$ one can rewrite $H_0 + V$ as:

$$H_0 = \begin{pmatrix} 2\Delta & up & 0 & 0 \\ up & -2\Delta & 0 & 0 \\ 0 & 0 & 0 & up \\ 0 & 0 & up & 0 \end{pmatrix} \quad V = \begin{pmatrix} \beta & 0 & -\mu & 0 \\ 0 & -\beta & 0 & -\mu \\ -\mu & 0 & \beta & 0 \\ 0 & -\mu & 0 & -\beta \end{pmatrix} \quad (3.22)$$

It's easy to see, subspace $\text{Span}(|+, +\rangle, |-, -\rangle)$ require no perturbation to obtain the eigenstates in the leading order. Indeed, diagonalizing the upper subblock of H_0 , one finds, that $E = \sqrt{(2\Delta)^2 + (up)^2}$. When the low energy states are the objects of interest ($E \sim g_{L,R}$), one finds, that $p = \pm \frac{i\Delta}{2u}$ in the leading order, and the corresponding eigenstates are $|+, +\rangle \pm i|-, -\rangle$. If

The another two eigenstates are a little bit more complicated. Diagonalizing the lower subblock of H_0 , one immediately finds, that $E = \pm up$. This corresponds to the fact, that H_0 is the version of H with a closed gap g on lower branch (see fig. 2.2,(e)), so in the zero order this states cannot form anything localized at all. To find them correctly, one needs to take into account the perturbation V and solve the secular equation using the following ansatz:

$$\psi = r_1 |+, +\rangle + r_2 |-, -\rangle + q_1 |+, -\rangle + q_2 |-, +\rangle \quad (3.23)$$

with $r_i \ll q_j$ for all pairs (i, j) . In the leading order (remember, that both E and up are of the order of $g_{L,R}$ now) this results to a couple of equations:

$$\begin{cases} \left(-E + B - \Delta - \frac{\mu^2}{2\Delta}\right) q_1 + upq_2 = 0 \\ upq_1 + \left(-E - B + \Delta + \frac{\mu^2}{2\Delta}\right) q_2 = 0 \end{cases} \quad (3.24)$$

recall, that at this precision $g = B - \Delta - \frac{\mu^2}{2\Delta}$ and find $E^2 = g^2 + u^2p^2$.

For this states the momenta are of the order of g/u , so it's reasonable to name them long-wave states. Than the states with momenta $\pm \frac{i\Delta}{2u}$ will be called mediumwave states. Now it's time to present this wavefunctions in original BdG basis. The expressions here are relevant only for the right lead and for $E > 0$. To find the wavefunctions in the left lead, the transform $\psi_L = \sigma_x\psi_R$

can be used, while for finding the negative energy states one can utilize electron-hole transform:

$\psi_{E<0} = \tau_y \sigma_y K \psi_{E>0}$ with K being a complex conjugation operator.

For $E > 2\Delta$ medium wave states are:

$$\psi_{medium}^{out, in} \Big|_{E>2\Delta} = \begin{pmatrix} 1 \\ \frac{E \mp \sqrt{E^2 - 4\Delta^2}}{2\Delta} \\ \frac{E \mp \sqrt{E^2 - 4\Delta^2}}{2\Delta} \\ 1 \end{pmatrix} e^{\frac{\pm ix \sqrt{E^2 - 4\Delta^2}}{u}} \quad (3.25)$$

For $E > 2\Delta$ medium wave states are:

$$\psi_{medium}^{grow, dec} \Big|_{E<2\Delta} = \begin{pmatrix} 1 \\ \frac{E \pm i\sqrt{4\Delta^2 - E^2}}{2\Delta} \\ \frac{E \pm i\sqrt{4\Delta^2 - E^2}}{2\Delta} \\ 1 \end{pmatrix} e^{\frac{\pm x \sqrt{4\Delta^2 - E^2}}{u}} \quad (3.26)$$

For $E > |g|$ longwave states are:

$$\psi_{long}^{out, in} \Big|_{E>g} = \begin{pmatrix} 1 \\ \frac{E \mp \sqrt{E^2 - g^2}}{g} \\ -\frac{E \mp \sqrt{E^2 - g^2}}{g} \\ -1 \end{pmatrix} e^{\pm \frac{ix \sqrt{E^2 - g^2}}{u}} \quad (3.27)$$

For $E < |g|$ longwave states are:

$$\psi_{long}^{grow, dec} \Big|_{E<g} = \begin{pmatrix} 1 \\ \frac{E \pm i\sqrt{g^2 - E^2}}{g} \\ -\frac{E \pm i\sqrt{g^2 - E^2}}{g} \\ -1 \end{pmatrix} e^{\pm \frac{x \sqrt{g^2 - E^2}}{u}} \quad (3.28)$$

3.5 Subgap states

To find the bound states one needs to make two linear combinations (each for its own wire) of decaying wave functions from (3.26) and (3.28) at $x = 0$ and put them into boundary condition (3.3). For the right wire they can be taken directly from (3.26), (3.28), while for the left wire they should be multiplied by σ_x from the left (see the beginning of section 3.4). These linear

combinations can be written as:

$$\tilde{\psi}_L = C_{medium}^L \sigma_x \psi_{medium}^{dec} + C_{long}^L \sigma_x \psi_{L,long}^{dec} \quad \tilde{\psi}_R = C_{medium}^R \psi_{medium}^{dec} + C_{long}^R \psi_{R,long}^{dec} \quad (3.29)$$

where $C_{medium}^L, C_{long}^L, C_{medium}^R, C_{long}^R$ are the undefined coefficients. Note, that the spinor ψ_{medium}^{dec} is the same for the left and for the right wires.

Putting these combinations into boundary condition 3.3, one can obtain four equations for these coefficients. If this system has a solution at energy E_0 , than there is a bound state with this energy. The condition of solvability can be written as:

$$\det F = 0 \quad (3.30)$$

where matrix F is given by:

$$F = \begin{pmatrix} M_L \sigma_x \psi_{medium}^{dec}, & M_L \sigma_x \psi_{L,long}^{dec}, & M_R \psi_{medium}^{dec}, & M_R \psi_{R,long}^{dec} \end{pmatrix} \quad (3.31)$$

As $E \sim g_{L,R} \ll \Delta$, the mediumwave spinor can be taken in it's low-energy form: In the most part of this work the low energy version: $\psi_{medium}^{dec} \approx (1, -i, -i, 1)^T$ will be used.

For dealing with ψ_{long}^{dec} it's convenient to introduce two quantities $\chi_{L,R}$:

$$\cosh \chi_{L,R} = \frac{g_{L,R}}{\sqrt{g_{L,R}^2 - E^2}} \quad \sinh \chi_{L,R} = \frac{E}{\sqrt{g_{L,R}^2 - E^2}} \quad (3.32)$$

If $g > 0$, the corresponding parameter χ is real and the monotonously growing with E . For $g < 0$ the corresponding is complex, but can be parametrized as $\chi = -\tilde{\chi} + i\pi$ with real and monotonous $\tilde{\chi}$.

With this parameters the spinors $\psi_{L(R),long}^{dec}$ at $x = 0$ can be written as:

$$\psi_{L(R),long}^{dec} = \begin{pmatrix} -\sinh \chi_{L(R)} - i \\ -\cosh \chi_{L(R)} \\ \cosh \chi_{L(R)} \\ \sinh \chi_{L(R)} + i \end{pmatrix} \quad (3.33)$$

This parametrization completes the toolset used for studying the subgap states.

3.5.1 The case of zero tunneling

Consider first the the equation (3.30) with $t = 0$. This corresponds to absolutely unpenetrable barrier, or, which is same, to independent wires ended with a vacuum. The computation of the

determinant in (3.30) becomes a rather easy problem and results in:

$$\det F \Big|_{t=0} = -16 (i \sinh(\chi_L) + \cosh(\chi_L) - 1) (i \sinh(\chi_R) + \cosh(\chi_R) - 1) \quad (3.34)$$

If both g_L, g_R are negative (triv-triv junction), this determinant cannot be equal to zero at all, as $\cosh \chi_{L,R}$ are also negative and the real part in each braces always non zero. If one of g_L, g_R (triv-top junction), say g_R there is only one solution at $E = 0$. If there both g_L, g_R (top-top junction) are positive, there are two solutions at $E = 0$.

This result proves, that the presence of Majorana mode in a isolated wire is defined only by the sign of g and justifies the notion of topology in this system.

3.5.2 Small tunneling

To take into account the tunneling effect one may decompose $\det F$ in t . Note, that there is no first order in t due to the structure of boundary condition (3.17). The decomposition can be written as:

$$\det F = d_0 + d_2 t^2 + \dots \quad (3.35)$$

where d_0 is given by (3.34). d_2 can be computed in a same way, but appears to be a rather complex formula. However, in tunneling limit the second correction in (3.35) should be much smaller than the first one, so the only values of E that should be considered are the ones with d_0 is close to zero.

For triv-triv junction there are no such points, so in the tunneling limit there are no bound states for this case.

For triv-top junction there is a solution for $E = 0$, which corresponds to $\chi_L = i\pi, \chi_R = 0$. Computing d_2 for this parameters, one finds that it's exactly zero, so there is no correction to Majorana energy — as at should be, as it's protected by a particle-hole symmetry.

For top-top junction the situation is more interesting. In that case there are two solutions at $E = 0$, which should split for nonzero t . Calculating d_2 at $E = 0$ and decomposing d_0 for small E , one finds:

$$d_0 = \frac{16E^2}{g_R g_L} \quad d_2 = -\frac{256t^2 \zeta^4}{(1 + \zeta^2)^2} \cos^2 \frac{\phi}{2} \quad (3.36)$$

Using, that $\zeta = 2bum \ll 1$, one can find the energy levels:

$$E_{1,2} = \pm 4t \zeta^2 \sqrt{g_R g_L} \cos \frac{\phi}{2} \quad (3.37)$$

this answer is relevant only if these level are well below the gaps: $t \zeta^2 \sqrt{g_R g_L} \ll \min [g_R, g_L]$.

3.6 Stationary supercurrent

The stationary supercurrent for a Josephson contact is defined by [27]:

$$I = -\frac{2e}{\hbar} \sum_p \tanh\left(\frac{\varepsilon_p}{2k_B T}\right) \frac{d\varepsilon_p}{d\varphi} - \frac{4e}{\hbar} k_B T \int_{cont.} d\varepsilon \log\left[2 \cosh\left(\frac{\varepsilon}{2k_B T}\right)\right] \frac{d\rho}{d\varphi} + \frac{2e}{\hbar} \frac{d}{d\varphi} \int dy \frac{|\Delta|^2}{|c|} \quad (3.38)$$

Here ε_p are the energies of the states localized near the barrier, ρ is the density of states and $c(\mathbf{r})$ is the interaction constant of the BCS theory, φ is a phase difference, k_B is a Boltzmann's constant and T is the temperature. The first term comes from the discrete spectra and the sum is taken over all states in it, the second term is the current from continuous spectra and the third term comes from inhomogeneity of the order parameter. As pointed in [27], despite being generally nonzero, this last term doesn't contribute when step-model functions Δ like in (2.4) are used.

After ommiting the third term and taking the low temperature limit one rewrites (3.38) as:

$$I = -\frac{2e}{\hbar} \sum_p \frac{d\varepsilon_p}{d\varphi} - \frac{2e}{\hbar} \int_{cont.} \varepsilon d\varepsilon \frac{d\rho}{d\varphi} \quad (3.39)$$

Here the only unknown quantity is the density of states. As there is a derivative over ϕ taken, one need to find the phase dependent part of ρ only. It can be done by using the relation between the density of states and the scattering matrix [28]:

$$\rho(\phi) = \frac{1}{2\pi i} \frac{\partial}{\partial \varepsilon} \log \det \hat{S} + const. \quad (3.40)$$

As was showed in the section 3.5, there are no undergap states in triv-top contact except Majorana state. But this state lays exactly on zero energy regardless of the phase difference, so the derivative in the first term of (3.39) will be zero and no supercurrent from the Majorana state is present.

The scattering matrix can be found with the help of boundary condition (3.17) and the results of section (3.4). It's dimension depends of the number of propagating modes at given energy. In this section only the triv-top. contact will be considered, while the scattering matrices and DOS for other types of contacts will be given in the appendix.

The process of building s-matrix is the following. Firstly, it's necessary to consider an energy and all the propagating wavefunctions at this energy. Among them there are wave functions, localized near the barrier ($\text{Imp} > 0$), propagating towards the barrier ($p < 0$), and propagating from

the barrier ($p < 0$). Let's denote these three sets as X_{local} , X_{in} and X_{out} . Each wavefunction ψ_i may contribute with it's own coefficient C_i — denote the vectors of the coefficients \vec{Y}_{local} , \vec{Y}_{in} and \vec{Y}_{out} . The s-matrix connects the coefficients from \vec{Y}_{in} to \vec{Y}_{out} in a following way:

$$\vec{Y}_{out} = \hat{S} \vec{Y}_{in} \quad (3.41)$$

to find a row of \hat{S} , one should be taken equal to unity, than take the functions from X_{local} , X_{out} and one chosen function $\Psi_{in,chosen}$ from X_{in} and make the linear combination of the form: $\Upsilon = \psi_{chosen}^{in} + c_1^{out} \Psi_1^{out} + c_2^{out} \Psi_2^{out} + \dots + c_1^{out} \Psi_1^{out} + c_2^{local} \Psi_2^{local} + \dots$. The one needs to act with the matrix 3.17 on Υ and obtain a set of equations for the coefficients c_i^{in} and c_i^{local} . This system should be solved, and the resulting coefficients c_i^{in} should form a row in \hat{S} , corresponding to $\Psi_{in,chosen}$. To construct the entire matrix \hat{S} , one should repeat this procedure for every function $\Psi_{in,chosen}$ in X_{in} .

The coefficients of \hat{S} generally depend on the normalization of the wavefunctions in X_{local} , X_{in} and X_{out} . To make the formula (3.40) valid, one must take the functions from X_{local} normalized to unity and the functions from X_{in} , X_{out} normalized to a flux[28]: $\langle \psi_{in,out} | v | \psi_{in,out} \rangle$ with v for our problem being $v = u \sigma_z \tau_z$.

Here some additional parameters will be used. When the given wavefunction is localized ($e < g$), θ -parametrization is used:

$$\theta_{L,R} : \quad \sin \theta_{L,R} = \frac{E}{g_{L,R}}, \quad \cos \theta_{L,R} > 0 \quad (3.42)$$

this parametrization is useful for both trivial and topological wires. When the wavefunction propagates ($E > g$), the η - or κ -parametrization is used, depending on the sign of g :

$$\eta_R : \quad \cosh \eta_R = \frac{E}{g_R}, \quad \sinh \eta_R > 0 \quad \kappa_L : \quad \cosh \kappa_L = \frac{E}{|g_L|}, \quad \sinh \kappa_L > 0 \quad (3.43)$$

The way to memorize it is that the η is used for a topological wire, whether the κ is used for a trivial wire. All the parameters $\theta_{L,R}$, κ_L and η_R are always real and positive when used.

As the dimension of s-matrix depends on the number of propagating modes, and thus on the energy, it's necessary to investigate different energy ranges separately.

For $E \ll \Delta$ one may use low energy limit of functions ψ_{medium}^{dec} : $\psi_{medium}^{dec} \approx (1, -i, -i, 1)^T e^{-\frac{2\Delta x}{u}}$ and also set $\gamma = -\frac{\pi}{2} \arcsin \frac{E}{\Delta} \approx -\frac{\pi}{2}$. When $E \sim \Delta$ one has to use γ as it is, and high energy of ψ_{low}^{dec} : $\psi_{low}^{dec} \approx (1, 0, 0, 1)^T e^{-\frac{Ex}{u}}$.

3.6.1 E between $|g_L|$ and g_R

Also recall, that the trivial wire is placed on the left of the barrier while the topological wire is on the right of it. There are two slightly distinct cases, which differ by relation between g_L and g_R .

The case $|g_L| > g_R$

For $g_R < E < |g_L|$ there is only one state in X_{in} , so the s-matrix has the dimension 1, so it's determinant coincides with it's only matrix element, which reads:

$$\det \hat{S} = -\frac{e^{\eta_R} + i}{1 + ie^{\eta_R}} - \frac{2i\zeta^4 t^2 e^{-i\varphi} (1 + e^{i\varphi})^2 (-1 + e^{i\theta_L}) (e^{2\eta_R} - 1)}{(\zeta^2 + 1)^2 (1 + e^{i\theta_L}) (e^{\eta_R} - i)^2} + O(t^3) \quad (3.44)$$

Using the (3.39) (3.40), one finds, that:

$$I = \frac{2e}{\hbar} \frac{4t^2 \zeta^4 \sin \varphi}{\pi} \left(\sqrt{g_L^2 - g_R^2} - \int_{g_R}^{|g_L|} dE \frac{\sqrt{E^2 - g_R^2}}{\sqrt{1 - \frac{E^2}{g_L^2} + 1}} \right) \quad (3.45)$$

The case $|g_L| < g_R$

When $|g_L| < E < g_R$ there is also only one state in X_{in} and the s-matrix is:

$$\det \hat{S} = \frac{e^{\kappa_L} - i}{-1 + ie^{\kappa_L}} - \frac{2i\zeta^4 t^2 e^{-i\varphi} (1 + e^{i\varphi})^2 (e^{2\kappa_L} - 1) (1 + e^{i\theta_R})}{(\zeta^2 + 1)^2 (e^{\kappa_L} + i)^2 (-1 + e^{i\theta_R})} + O(t^3) \quad (3.46)$$

Again with the help of (3.39) (3.40), one finds, that:

$$I = \frac{2e}{\hbar} \frac{4t^2 \zeta^4 \sin \varphi}{\pi} \left(\sqrt{g_R^2 - g_L^2} - g_R \int_{|g_L|}^{g_R} \frac{dE}{E^2} \sqrt{E^2 - g_L^2} \left(\sqrt{1 - \frac{E^2}{g_R^2} + 1} \right) \right) \quad (3.47)$$

3.6.2 E is greater than both $|g_L|$ and g_R and much smaller than Δ

Here there are two states in X_{in} – one in the right wire and one in the left, so the s-matrix has the dimension equal to two. Arranging it's elements in the following order:

$$\hat{S} = \begin{pmatrix} r_{LL} & t_{LR} \\ t_{RL} & r_{RR} \end{pmatrix} \quad (3.48)$$

one gets:

$$r_{LL} = \frac{e^{\kappa_L} - i}{-1 + ie^{\kappa_L}} + \frac{2\zeta^4 t^2 e^{-i\varphi} (1 + e^{i\varphi})^2 (e^{2\kappa_L} - 1) (e^{\eta_R} + i)}{(\zeta^2 + 1)^2 (e^{\kappa_L} + i)^2 (-1 - ie^{\eta_R})} + O(t^3) \quad (3.49)$$

$$r_{RR} = -\frac{e^{\eta_R} + i}{1 + ie^{\eta_R}} + \frac{2\zeta^4 t^2 e^{-i\varphi} (1 + e^{i\varphi})^2 (e^{\kappa_L} - i) (e^{2\eta_R} - 1)}{(\zeta^2 + 1)^2 (-1 + ie^{\kappa_L}) (e^{\eta_R} - i)^2} + O(t^3) \quad (3.50)$$

$$t_{LR} = \frac{2\zeta^2 t e^{-i\varphi} (1 + e^{i\varphi}) \sqrt{(e^{2\kappa_L} - 1) (e^{2\eta_R} - 1)}}{(\zeta^2 + 1) (e^{\kappa_L} + i) (e^{\eta_R} - i)} + O(t^3) \quad (3.51)$$

$$t_{RL} = -\frac{2t\zeta^2 (1 + e^{i\varphi}) \sqrt{(e^{2\kappa_L} - 1) (e^{2\eta_R} - 1)}}{(\zeta^2 + 1) (e^{\kappa_L} + i) (e^{\eta_R} - i)} + O(t^3) \quad (3.52)$$

The computation of supercurrent is again made with the (3.39) (3.40). Introducing :

$$g_{max} = \begin{cases} g_R, & g_R > |g_L| \\ g_L, & |g_L| > g_R \end{cases} \quad g_{min} = \begin{cases} g_R, & g_R < |g_L| \\ g_L, & |g_L| < g_R \end{cases} \quad s_g = \begin{cases} 1, & g_R > |g_L| \\ -1, & g_R < |g_L| \end{cases} \quad (3.53)$$

one finds:

$$I \sim \frac{2e}{\hbar} \frac{4t^2 \zeta^4 \sin \varphi}{\pi} \times \left(s_g \sqrt{g_{max}^2 - g_{min}^2} - g_{max} g_{min} \int_{g_{max}}^{\Delta} \frac{dE}{E^2} \left(\frac{\sqrt{E^2 - g_{max}^2}}{g_{max}} + \frac{\sqrt{E^2 - g_{min}^2}}{g_{min}} \right) \right) \quad (3.54)$$

it's important to note, that this computation is irrelevant for $E \sim \Delta$, so Δ here acts like high energy cutoff.

3.6.3 E is near and below Δ

To make the estimate for the supercurrent at energies $E \lesssim \Delta$ high energy versions of ψ_{low} can be used, so the system forgets about g_L and g_R and becomes effectively symmetric. Taking the notation from (3.48), find:

$$r_{LL} = r_{RR} = e^{i\gamma} + \zeta^2 t^2 e^{-i\varphi} \left(\frac{(-1 + e^{2i\gamma})^2 (1 + e^{i\varphi})^2}{e^{i\theta} - e^{i\gamma}} + 2e^{i\gamma} (e^{2i(\gamma+\varphi)} + e^{2i\gamma} - 2e^{i\varphi}) \right) + O(t^3) \quad (3.55)$$

$$t_{RL} = -t_{RL} = i\zeta t (1 + e^{2i\gamma}) (-1 + e^{i\varphi}) + O(t^3) \quad (3.56)$$

Using (3.39) (3.40), one may find (3.39) (3.40)

$$I \sim \frac{e}{\hbar} \zeta^2 t^2 \Delta \quad (3.57)$$

3.6.4 Analysing the results

From (3.47) and (3.45) one may see, that the current coming from the states between g_L and g_R has a multiplier of the order $g_{L,R}$. The current from the states above g_{max} , but close to it, can be estimated with (3.54). It has the multiplier $g_{min} \log \frac{\Delta}{g_{max}}$. The current states near Δ according to (3.57) is proportional to Δ . Thus one may deduce that the current from the low energy states is negligible compared with the current from the states near Δ .

This is similar to the result of short Josephson junction with some bound state below the gap. It can be shown, that in that case the current from the subgap state will be proportional to the same quantity as (3.57).

Chapter 4

Ionization

In this chapter the model, previously presented is modified to allow the ionization processes. The main goal here is to find the ionization rate of a Majorana state, when the typical size of the photon is much smaller, than the gap in the spectrum. Only regime with $|g_L| \ll g_R$ is considered — even though the ionization for this condition is factorized, it contains its own nontrivial physics with a number of different subregimes.

4.1 Introducing the perturbation

To study the ionization behavior of the system, it's necessary must modify the model considered in chapter 2. It's reasonable to assume, that this perturbation will be present as an alternating voltage applied to the junction. This may alter the Hamiltonian (2.3) in two ways — by the modification of the chemical potentials μ_L, μ_R and by making the superconducting phase difference $\varphi = \phi_R - \phi_L$ time dependent. The second effect can be described by a Josephson relation:

$$U(t) = \frac{\hbar}{2e} \frac{\partial \varphi(t)}{\partial t} \quad (4.1)$$

The ionization voltage is assumed to be small compared to other energy parameters of the system, but this smallness is present in both effects. However, if the frequency ω of the voltage is also small, the perturbation induced by the second effect will have additional big multiplier $\frac{\Delta}{\omega}$ and will be much more important than the first. In this chapter only this regime is taken under consideration.

The time dependence of phase difference is introduced as:

$$\varphi(t) = \varphi_0 + \alpha \cos \omega t \quad (4.2)$$

where φ_0 is an initial time independent phase difference and α is an amplitude of phase oscillations.

As was shown in section 3.3, there exists a gauge transform U_ϕ , which may redistribute the phase difference between the wires, so the phase in a given wire can take any value. This ambiguity just reflects a fact, that only phase difference φ is an observable quantity, but not the phases ϕ_L, ϕ_R separately. However when treating the time dependent $\phi(t)$, where the oscillating

phase is present. Moreover, the voltage frequency ω is assumed to be much smaller than not only the superconducting gap Δ , but the spectrum gaps in both wires: $\omega \ll g_R, |g_L|$

The correct answer is that both left and right wires should get equal time-dependent phase with different signs: $\phi_L = -\frac{\varphi_0}{2} - \frac{\alpha}{2} \cos \omega t$, $\phi_R = \frac{\varphi_0}{2} + \frac{\alpha}{2} \cos \omega t$. Thus the superconducting terms in the wire Hamiltonians alter: $\Delta_{\pm \frac{\varphi}{2}} \rightarrow \Delta_{\pm \frac{\varphi}{2} \pm \frac{\alpha}{2} \cos \omega t}$. Decomposing them in small α one can explicitly write the perturbation and try to compute the ionization rate. However this way appears to be quite difficult as the overlaps of all the states present in both wires and at first it seems that the Majorana states has too many ways to ionize. To avoid this difficulty, the tunnel Hamiltonian approach is used.

4.2 Tunnel Hamiltonian approach

The main idea of this method is to hide all the time dependence and the tunnel effect in one single operator. The local goal is to write the Hamiltonian as $H = H_L + H_R + H_T$, where $H_{L,R}$ are the Hamiltonians of the left and right wire without any contact (corresponding to zero tunneling: $t = 0$), and H_T is a tunnel Hamiltonian both containing the time dependence and mixing the wavefunctions from different wires.

Here the following notation is used. The Hamiltonians H_L , H_R and H_T are 8x8 matrices in combined Nambu-Gorkov and LR-space. In LR-space they have the following form:

$$H_L = \begin{pmatrix} h_L & 0 \\ 0 & 0 \end{pmatrix}_{LR}, \quad H_R = \begin{pmatrix} 0 & 0 \\ 0 & h_R \end{pmatrix}_{LR}, \quad H_T = \begin{pmatrix} 0 & h_T^\dagger \\ h_T & 0 \end{pmatrix}_{LR} \quad (4.3)$$

The spinors with four components are corresponding to the unperturbed wavefunctions and are denoted as $|\gamma_0\rangle$, for the Majorana state and $|\varepsilon, L_0\rangle, |\varepsilon, R_0\rangle$ for the contentious spectra in the left and in the right wires respectfully, and the corrections are denoted as $|\gamma_1\rangle, |\varepsilon, L_1\rangle, |\varepsilon, R_1\rangle$. These wavefunctions can be found in the appendix A. In the combined space of dimension 8 this spinors are:

$$\Psi_\gamma = \begin{pmatrix} 0 \\ |\gamma_0\rangle \end{pmatrix}_{LR} + \begin{pmatrix} |\gamma_1\rangle \\ 0 \end{pmatrix}_{LR} + \dots \quad (4.4)$$

$$\Psi_R = \begin{pmatrix} 0 \\ |\varepsilon, R_0\rangle \end{pmatrix}_{LR} + \begin{pmatrix} |\varepsilon, R_1\rangle \\ 0 \end{pmatrix}_{LR} + \dots \quad (4.5)$$

$$\Psi_L = \begin{pmatrix} |\varepsilon, L_0\rangle \\ 0 \end{pmatrix}_{LR} + \begin{pmatrix} 0 \\ |\varepsilon, L_1\rangle \end{pmatrix}_{LR} + \dots \quad (4.6)$$

The correct way to write H_T is to make it restoring the corrections from appendix A. To do so, one may write the unperturbed Green function of the system as:

$$G_0(E) = \frac{1}{E + i0} \begin{pmatrix} 0 & 0 \\ 0 & |\gamma_0\rangle\langle\gamma_0| \end{pmatrix}_{LR} + \int_{g_L}^{\infty} \frac{d\varepsilon}{N_L(\varepsilon)} \frac{1}{E + i0 - \varepsilon} \begin{pmatrix} |\varepsilon, L_0\rangle\langle\varepsilon, L_0| & 0 \\ 0 & 0 \end{pmatrix}_{LR} + \int_{g_l}^{\infty} \frac{d\varepsilon}{N_R(\varepsilon)} \frac{1}{E + i0 - \varepsilon} \begin{pmatrix} 0 & 0 \\ 0 & |\varepsilon, R_0\rangle\langle\varepsilon, R_0| \end{pmatrix}_{LR} \quad (4.7)$$

with $N_{L,R}$ from (A.2). The corrections for the spinors should be calculated as:

$$\Psi_1(E) = G_0(E) H_T \Psi_0(E) \quad (4.8)$$

So, for the different states:

$$|\gamma_1\rangle = \int_{g_L}^{\infty} \frac{d\varepsilon}{N_L(\varepsilon)} \frac{1}{-\varepsilon + i0} |\varepsilon, L_0\rangle \langle\varepsilon, L_0| h_t |\gamma_0\rangle \quad (4.9)$$

$$|E + i0, R_1\rangle = \int_{g_L}^{\infty} \frac{d\varepsilon}{N_L(\varepsilon)} \frac{1}{E - \varepsilon + i0} |\varepsilon, L_0\rangle \langle\varepsilon, L_0| h_t |E R_0\rangle \quad (4.10)$$

$$|E + i0, L_1\rangle = \frac{1}{E + i0} |\gamma_0\rangle \langle\gamma_0| h_t^\dagger |E, L_0\rangle + \int_{g_l}^{\infty} \frac{d\varepsilon}{N_R(\varepsilon)} \frac{1}{E - \varepsilon + i0} |\varepsilon R_0\rangle \langle\varepsilon, R_0| h_t^\dagger |E, L_0\rangle \quad (4.11)$$

Now, multiplying the third equation by $\langle\gamma_0|$ and $\langle\varepsilon, R_0|$, find:

$$\langle\gamma_0|E + i0, L_1\rangle = \frac{1}{E + i0} \langle\gamma_0| h_t^\dagger |E, L_0\rangle \quad (4.12)$$

$$\langle\varepsilon, R_0|E + i0, L_1\rangle = \frac{1}{E - \varepsilon + i0} \langle\varepsilon, R_0| h_t^\dagger |E, L_0\rangle \quad (4.13)$$

The l.h.s. of both equations above can be found explicitly with the help of appendix A. The result yields:

$$\langle\gamma_0| h_t^\dagger |E, L_0\rangle = 4\sqrt{ug_R}\zeta^2 t \left(e^{i\frac{\phi}{2}} + e^{-i\frac{\phi}{2}} \right) f\left(\frac{E}{|g_L|}\right) \quad (4.14)$$

$$\langle\varepsilon, R_0| h_t^\dagger |E, L_0\rangle = -16u\zeta^2 t \left(e^{i\frac{\phi}{2}} + e^{-i\frac{\phi}{2}} \right) f\left(\frac{E}{|g_L|}\right) f\left(\frac{\varepsilon}{g_R}\right) \quad (4.15)$$

where $f(x) = \sqrt{x^2 - 1} (x + \sqrt{x^2 - 1})$. The fact, that all energy dependences here are described by a single function $f(x)$ insinuates that, maybe it's possible to make this calculations in a more beautiful way.

4.3 Ionization rate for $g_R \gg |g_L|$

4.3.1 Time dependence of perturbation

To obtain the ionization rate one should treat H_T as perturbation. For unperturbed system, described with $H_0 = H_R + H_L$ the electrons cannot get from wire to another, but H_T allows these processes, so the ionization can be described as a set of jumps from right to left wire (see fig. 4.1)

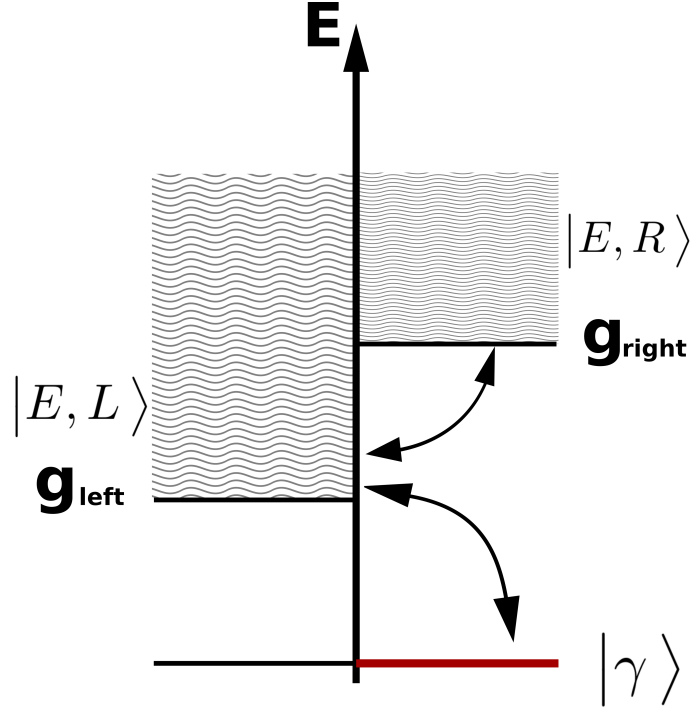


Figure 4.1: Ionization processes in terms of tunnel Hamiltonian

The ionization rate can be calculated with the help of (B.23). To use this formula, one should decompose the perturbation in Fourier series, as was done for (B.10). From (4.14) one finds, that $V = H_T \propto \cos \frac{\varphi(t)}{2}$ with $\varphi = \phi_0 + \alpha \cos \omega t$. Using $\alpha \ll 1$ we write:

$$\begin{aligned} e^{i\varphi/2} + e^{-i\varphi/2} &\simeq e^{i\frac{\varphi_0}{2}} \sum_n \frac{(i\alpha/2)^n}{2^n n!} (e^{in\omega t} + e^{-in\omega t}) + c.c = \\ &= \sum_n \frac{\alpha^n}{2^{2n} n!} (e^{in\omega t} + e^{-in\omega t}) 2 \cos \left(\frac{\varphi_0}{2} + n \frac{\pi}{2} \right) \end{aligned} \quad (4.16)$$

so that $V_n = V_0 A_n$ with $A_n = \frac{\alpha^n}{2^{2n-1} n!} \cos \left(\frac{\varphi_0}{2} + n \frac{\pi}{2} \right)$.

According to (4.14) and (4.15):

$$\langle \gamma | V_0 | E \rangle = 4\sqrt{ug_R} \zeta^2 t f \left(\frac{E}{|g_L|} \right) \quad (4.17)$$

Here the focus is on the case where the topological gap is much larger than the trivial one. In this case, the right continuum has high energies and does not participate in the ionization process. Indeed,

$$VG_\epsilon V = \frac{V|\gamma\rangle\langle\gamma|V}{\epsilon} + \int_{|E_R|>g_R} \frac{V|E_R\rangle\langle E_R|V}{\epsilon - E_R} \frac{dE_R}{N_R(E_R)} \quad (4.18)$$

When $g_R \gg \epsilon \sim g_L$, the second term can be neglected. Then, the product $\dots V_n G V_{n'} G V_{n''} \dots$ factorizes into individual number-factors of the form $\langle\gamma|V_n G V_m|\gamma\rangle$.

4.3.2 Factorizing $w_{\mathcal{E}}$

Each entry in the sum within $w_{\mathcal{E}}$ is a product of operators of the type $\dots V G V G V \dots$. In the limit we are now interested in, in the right wire only the Majorana mode is relevant. This means that the whole thing decomposes into a product of $J_{nm} \equiv \langle\gamma|V_n|G_E|V_m|\gamma\rangle$, and the ionization rate is proportional to:

$$\sqrt{\mathcal{I}} \propto \sum_N \sum_{\{n_i\}_M^N} \prod_{i=1}^N J_{n_i n_{i+1}} \quad (4.19)$$

Here the N has the meaning of total number of absorbed photons, M is the closet to $\frac{|g_L|}{\omega}$ integer, and the second sum is taken over all sets $\{n_i\}_M^N$ such that there are N items in that set and $\sum_i^N n_i = M$. The n, m -dependence factors out so that $J_{nm} = A_n A_m^* J_0$ where:

$$J_0(E) = \langle\gamma|V_0 G(E) V_0|\gamma\rangle \equiv \int_{cont.} \frac{|\langle\gamma|V_0|\epsilon\rangle|^2}{E - \epsilon} \frac{d\epsilon}{N_L(\epsilon)} \quad (4.20)$$

However on each ionization step the particle can move a state with energy E or $-E$. Taking this into account, one gets:

$$J_0(E) = 2E \int_{|g_L|}^{\infty} \frac{|\langle\gamma|V_0|\epsilon\rangle|^2}{E^2 - \epsilon^2} \frac{d\epsilon}{f(\epsilon)} \quad (4.21)$$

recalling (4.17), obtain:

$$J_0(E) = ET \frac{[-1 + \sqrt{1 - \lambda^2}]}{\lambda^2} \quad (4.22)$$

where $\lambda = \frac{E}{|g_L|}$, $T = \frac{g_R(\zeta^2 t)^2}{|g_L|}$.

Thus, the elementary block in our product becomes:

$$\begin{aligned} \frac{J_{nm}}{E + n\omega} &= A_n A_m \frac{J_0}{E + n\omega} \simeq A_n A_m T \frac{[-1 + \sqrt{1 - \lambda^2}]}{\lambda^2} = \\ &= \left(\frac{\alpha}{4}\right)^{n+m} B_n B_m^* T \frac{[-1 + \sqrt{1 - \lambda^2}]}{\lambda^2} \end{aligned} \quad (4.23)$$

where the parts that yield $(\alpha/4)^{\varepsilon/\omega}$ for any trajectory and thus are factored out, as these parts do not affect summation and optimization. Thus one has $B_n B_m^* T \frac{[-1 + \sqrt{1 - \lambda^2}]}{\lambda^2}$ to optimize.

Now consider a slice of the ionization process, i.e. a part of the full ionization product, which runs from energy E to $E + \Delta E$ where $\Delta E = M\omega$ with a large M . One can assume that within that process, a large number $2N$ of photons is absorbed, but energy does not change significantly, $\Delta E \ll E$, so that λ can be considered a constant within that process. Denoting:

$$T_\lambda = -4T \frac{[-1 + \sqrt{1 - \lambda^2}]}{\lambda^2} \quad (4.24)$$

Then, one finds, that the ionization rate is $\mathcal{I} \propto \mathcal{J}^2$ where:

$$\mathcal{J} \equiv \sum_{\{n\}_N^M} \prod_{i=1}^N \frac{J_{n_i m_i}}{E} = \left(\frac{\alpha}{4}\right)^M \sum_{\{n\}_{2N}^M} (-T_\lambda)^{\frac{N}{2}} \prod_{i=1}^N \frac{\cos\left(\frac{\varphi_0}{2} + \frac{\pi n_{2i}}{2}\right)}{n_i!} \quad (4.25)$$

So to obtain the ionization rate up to a preexponential constant, one should compute \mathcal{J} .

4.3.3 Using multinomial formula

The first step to deal with (4.25) is to rewrite the product of cosines using multinomial formula:

$$\frac{d^n}{dx^n} \prod_i f_i(x) = \sum_{\sum_i k_i = n} \binom{n}{k_1, k_2, \dots, k_n} \prod_i f_i^{(k_i)} \quad (4.26)$$

For the cosing product it can be applied in a following way:

$$\sum_{\{n\}_N^M} \prod_{i=1}^N \frac{\cos\left(\chi + \frac{\pi n_i}{2}\right)}{n_i!} = \sum_{\{n\}_N^M} \prod_{i=1}^N \frac{D_\chi^{n_i}}{n_i!} \cos \chi = \frac{1}{M!} D_\chi^M \cos^N \chi \quad (4.27)$$

Then some algebra should be used:

$$\begin{aligned} \frac{1}{M!} D_\chi^M \cos^N \chi &= \frac{1}{M! 2^N} D_\chi^M \sum_{k=0}^N C_k^N e^{i\chi(N-2k)} = \\ &= \frac{1}{M! 2^N} \sum_{k=0}^N C_k^N (i(N-2k))^M e^{i\chi(N-2k)} = \frac{e^{i\chi N + iM\pi/2}}{M! 2^N} \sum_{k=0}^N C_k^N (N-2k)^M e^{-2ki\chi} \quad (4.28) \end{aligned}$$

Now, in the sum, the ratio of consecutive summands is $\frac{a_{k+1}}{a_k} = \frac{C_{k+1}^N}{C_k^N} \left(\frac{N-2k-2}{N-2k} \right)^M$. For $k < N/2$ both factors here are decreasing, so the largest ratio is $\frac{a_1}{a_0} = N \left(\frac{N-2}{N} \right)^M \simeq N e^{-2M/N}$. The most important terms in this sum define in which regime the system is and what the ionization rate would be.

One can anticipate that the typical (i.e. most important) value of N is given by $N_* = \frac{2M}{n_*}$ with $n_* = \log \frac{1}{T_\lambda}$. It can be shown from considering the action $s = \log \frac{1}{T_\lambda} - \frac{2}{2M}$ which appears in this sum. Taking $N = N_*$ one can rewrite the condition $\left| \frac{a_1}{a_0} \right| \ll 1$ as $\frac{2M}{n_*} \ll e^{n_*}$. This condition separates two regimes of the system — pure Andreev regime, when only the first and the last terms in the sum are relevant, and the Andreev+Normal regime, when other terms should be taken into account.

4.3.4 Pure Andreev regime

When $\frac{2M}{n_*} \ll e^{n_*}$ the sum (4.28) can be rewritten as:

$$\mathcal{J} \approx \left(\frac{\alpha}{4} \right)^M \sum_N (-T_\lambda)^{N/2} \frac{N^M}{M! 2^N} \times 2 \cos \left(\chi N + \frac{M\pi}{2} \right) \quad (4.29)$$

The preexponent is not the object of interest, while the fixed parity of N should be taken into account (it is fixed since the continuum state is available only on the left side of the junction).

Replace $N = 2K$ and obtain:

$$\begin{aligned} I_M &= \left(\frac{\alpha}{4} \right)^M \sum_{K=1}^{\infty} (-T_\lambda)^K \frac{(2K)^M}{M! 2^{2K}} \times 2 \cos \left(\phi_0 K + \frac{M\pi}{2} \right) = \\ &= \frac{2}{M!} \left(\frac{\alpha}{4} \right)^M \Re \left[i^M \sum_K (-T_\lambda)^K \frac{(2K)^M}{2^{2K}} e^{i\phi_0 K} \right] = \\ &= \frac{2^{M+1}}{M!} \left(\frac{\alpha}{4} \right)^M \Re \left[i^M \text{Li}_{-M} \left(\frac{T_\lambda}{4} e^{i(\phi_0 + \pi)} \right) \right] \quad (4.30) \end{aligned}$$

The polylogarithmic function can be rewritten in the following useful way

$$\text{Li}_s(e^\mu) = \Gamma(1-s) \sum_{r \in \mathbb{Z}} (2r\pi i - \mu)^{s-1}$$

Substituting, we get

$$\text{Li}_{-M} \left(\frac{T_\lambda}{4} e^{i(\phi_0 + \pi)} \right) = \Gamma(1 + M) \sum_{r \in \mathbb{Z}} \left(i[2r\pi - \pi - \phi_0] + \ln \frac{4}{T_\lambda} \right)^{-M-1}$$

Denoting $\ln \frac{4}{T_\lambda} = n_\lambda$ we have the ratio of consecutive terms in the sum (assuming they are not too far from the largest term):

$$\left| \frac{a_{r+1}}{a_r} \right| \sim \left(\frac{n_\lambda^2 + (\gamma_r + 2\pi)^2}{n_\lambda^2 + \gamma_r^2} \right)^{-1-M} \sim \left(1 + \frac{2\pi(2\pi + 2\gamma_r)}{n_\lambda^2 + \gamma_r^2} \right)^{-M} \sim \exp \left[\frac{4\pi M(\pi + \gamma_r)}{n_\lambda^2} \right]$$

where $\gamma_r = i(2r\pi - \pi - \phi_0)$. There are two values of r for which $|\pi + \gamma_r|$ is smallest, for the rest it is not smaller than 2π so that the rest of the terms are smaller by at least

$$\exp \left[-\frac{8\pi^2 M}{n_\lambda^2} \right]$$

Subcase

$$\exp \left[\frac{8\pi^2 M}{n_\lambda^2} \right] \gg 1$$

in which case the sum over r is dominated by the two largest terms (typically by just one term except for the case when ϕ_0 is close to zero). We dictate $-\pi < \phi_0 < \pi$ so that the two dominating terms correspond to $r = 0, 1$. We have in that limit

$$\text{Li}_{-M} \left(\frac{T_\lambda}{4} e^{i(\phi_0 + \pi)} \right) \simeq M! \left(\frac{1}{(n_\lambda + i(\pi - \phi_0))^{M+1}} + \frac{1}{(n_\lambda + i(-\pi - \phi_0))^{M+1}} \right)$$

and thus

$$I_M = 2 \left(\frac{\alpha}{2} \right)^M \Re \left[i^M \left(\frac{1}{(n_\lambda + i(\pi - \phi_0))^{M+1}} + \frac{1}{(n_\lambda + i(-\pi - \phi_0))^{M+1}} \right) \right]$$

We have

$$[n_\lambda + i(\pi - \phi_0)]^{M+1} = [n_\lambda^2 + (\pi - \phi_0)^2]^{\frac{M+1}{2}} e^{i(M+1) \arctan \frac{\pi - \phi_0}{n_\lambda}}$$

and

$$\begin{aligned} I_M &= 2 \left(\frac{\alpha}{2} \right)^M \Re \left[\frac{e^{\frac{iM\pi}{2} - i(M+1) \arctan \frac{\pi - \phi_0}{n_\lambda}}}{[n_\lambda^2 + (\pi - \phi_0)^2]^{\frac{M+1}{2}}} + \frac{e^{\frac{iM\pi}{2} + i(M+1) \arctan \frac{\pi + \phi_0}{n_\lambda}}}{[n_\lambda^2 + (\pi + \phi_0)^2]^{\frac{M+1}{2}}} \right] = \\ &= 2 \left(\frac{\alpha}{2} \right)^M \left[\frac{\cos \left(\frac{M\pi}{2} - (M+1) \arctan \frac{\pi - \phi_0}{n_\lambda} \right)}{[n_\lambda^2 + (\pi - \phi_0)^2]^{\frac{M+1}{2}}} + \frac{\cos \left(\frac{M\pi}{2} + (M+1) \arctan \frac{\pi + \phi_0}{n_\lambda} \right)}{[n_\lambda^2 + (\pi + \phi_0)^2]^{\frac{M+1}{2}}} \right] \end{aligned}$$

This contains some complicated oscillations but within exponential accuracy we may write

$$I_M \sim \exp M \left[\ln \frac{\alpha}{2} - \frac{1}{2} \ln(n_\lambda^2 + (\pi - |\varphi_0|)^2) \right]$$

This is almost the final formula for the ionization amplitude. To finalize it, we have to replace the action at fixed n_λ by an integration over λ to account for the slowly changing energy of the quasiparticle. However, it is unclear, what is required of M, n_* to allow such a procedure. The procedure assumes that we can roughly write $I_M = \prod_j I_{M_j}(\lambda_j)$ where the full process is split into layers counted by j where within each layer energy is roughly the same and $\sum M_j = M$, but M_j is relatively large (so that N_j remains large). Hypothetically, if our principal conditions are met (the ones that limit the sum to highest harmonics and allow the use of asymptotics for Li) then we can split M into layers which individually obey the same limits. Therefore, in the mathematical limit the procedure seems correct, but it is hard to tell, what accuracy it has. We have

$$\begin{aligned} s_\lambda &= \int_0^1 \ln(n_\lambda^2 + (\pi - |\varphi_0|)^2) d\lambda = \int_0^1 \ln(\ln(\frac{4}{T_\lambda})^2 + (\pi - |\varphi_0|)^2) d\lambda \\ &= \int_0^1 \ln \left(\left[\ln \frac{\lambda^2}{T_0(1 - \sqrt{1 - \lambda^2})} \right]^2 + (\pi - |\varphi_0|)^2 \right) d\lambda \end{aligned}$$

Calculation of the λ -integral:

$$\int_0^1 \ln(n_\lambda^2 + (\pi - |\varphi_0|)^2) d\lambda = \int_0^1 \left(2 \ln n_\lambda + \frac{(\pi - |\varphi_0|)^2}{n_\lambda^2} \right) d\lambda$$

Separately we find:

$$\int_0^1 \ln n_\lambda d\lambda = \ln \frac{1}{T} + \int_0^1 \ln \frac{\lambda^2}{1 - \sqrt{1 - \lambda^2}} d\lambda = \ln \frac{1}{T} + \frac{\pi}{2} - 1.$$

For the second integral we have

$$\int_0^1 \frac{1}{n_\lambda^2} d\lambda = \int_0^1 \frac{1}{\left[\ln \frac{1}{T} + \ln \frac{\lambda^2}{1 - \sqrt{1 - \lambda^2}} \right]^2} d\lambda = \frac{1}{(\ln \frac{1}{T})^2} + O\left(\frac{1}{(\ln \frac{1}{T})^3}\right)$$

Thus, we get

$$s_\lambda = 2 \ln \frac{1}{T} + \pi - 2 + \frac{(\pi - |\varphi_0|)^2}{(\ln \frac{1}{T})^2} + O\left(\frac{1}{(\ln \frac{1}{T})^3}\right)$$

and the final result in this limit (only pure MAR (multiple Andreev reflections)) is:

$$P = \exp \left[-\frac{g_L}{\omega} \left(2 \ln \frac{2}{\alpha} + 2 \ln \ln \frac{1}{T} + \pi - 2 + \frac{(\pi - |\varphi_0|)^2}{(\ln \frac{1}{T})^2} + O \left(\frac{1}{(\ln \frac{1}{T})^3} \right) \right) \right]$$

$$(\ln \frac{1}{T})^2 \ll \frac{g_L}{\omega} \ll (\ln \frac{1}{T})^2 e^{1/T}$$

and in the second regime,

$$P = \exp \left[-\frac{g_L}{\omega} \left(2 \ln \frac{2}{\alpha} + 2 \ln \ln \frac{1}{T} + \pi - 2 + o(1) \right) \right]$$

$$(\ln \frac{1}{T})^2 \ll \frac{g_L}{\omega}$$

This includes the previous answer. The $o(1)$ is to be determined.

Finally, in the case where $n_* \ll M \ll n_*^2$ I do Poisson to calculate Li and find that it behaves strangely: I get $e^{-M \ln n_\lambda - \frac{1}{2} \frac{M^2}{n_\lambda^2} n_\lambda^2 / M + \text{corr.}}$ where M/n_λ denotes the fractional part of the number (from $-1/2$ to $1/2$). The number within changes quickly with λ and therefore $^2 \rightarrow \langle^2 \rangle = 1/12$. Then, we get

$$P = \exp \left[-\frac{g_L}{\omega} \left(2 \ln \frac{2}{\alpha} + 2 \ln \ln \frac{1}{T} + \pi - 2 \right) + \frac{1}{12} \frac{(\ln \frac{1}{T})^2}{g_L/\omega} + o \left(\frac{(\ln \frac{1}{T})^2}{g_L/\omega} \right) \right] \quad (4.31)$$

$$(\ln \frac{1}{T}) \ll \frac{g_L}{\omega} < (\ln \frac{1}{T})^2 \quad (4.32)$$

Pure Andreev regime regime: intermediate case: fixed photon number

Above we considered $M \gg n_*$ which lead to a simple asymptotic of the function $\text{Li}_{-M}(e^{-n_* + i(\phi_0 + \pi)})$. There is also the intermediate case where $n_* \ll M \ll n_*^2$. In this case the dominating term(s) have large index K , but the gaussian envelope is very narrow, with a width $\ll 1$ which means that the full series is dominated by a single term (this is in full agreement with the fact that the second form of Li is now wide, i.e. converges over a large number of r -terms). It is easy to show that the optimal term has the integer index K_0 closest to the real saddle-point $K_* = M/n_*$. We write

$$K_* = K_0 + \xi, \quad \text{with} \quad \xi \in (-\frac{1}{2}, \frac{1}{2})$$

Then, omitting the complex phase, we write

$$\begin{aligned} \text{Li}_{-M}(e^{-n_*+i(\phi_0+\pi)}) &\approx a_{K_0} \propto e^{-n_*(K_*-\xi)+M \ln(K_0-\xi)} = \\ &= e^{-M+n_*\xi+M \ln \frac{M}{n_*}+M \ln(1-\frac{\xi n_*}{M})} = e^{-M+M \ln \frac{M}{n_*}-\frac{\xi^2 n_*^2}{2M}+O\left(\frac{n_*^3}{M^2}\right)} \end{aligned}$$

Substituting this result for the Li function we obtain in this regime (to exponential accuracy)

$$I \sim \frac{1}{M!} \left(\frac{\alpha}{2}\right)^M e^{-M+M \ln \frac{M}{n_*}-\frac{\xi^2 n_*^2}{2M}+O\left(\frac{n_*^3}{M^2}\right)} = e^{-M \ln \frac{2}{\alpha}-M \ln n_*-\frac{\xi^2 n_*^2}{2M}+O\left(\frac{\xi^3 n_*^3}{M^2}\right)}$$

and for the probability we write:

$$P_2 = \exp \left[-M \left(2 \ln \frac{2}{\alpha} + 2 \ln n_* \right) - \left\{ \frac{M}{n_*} \right\}^2 \frac{n_*^2}{M} + O \left(\frac{n_*^3}{M^2} \right) \right], \quad n_* \ll M \ll n_*^2$$

4.3.5 Andreev+Normal regime

For completeness, let us also consider the case $M/N \ll \log N$. In this case the sum over k is not defined by the two edge terms. We write:

$$\sum_{k=0}^N C_k^N (N-2k)^M e^{-2ki\chi} = \sum_{k=0}^N e^{-S_0(k)-2ki\chi}$$

where the action S_0 is

$$\begin{aligned} S_0 &= -\ln C_k^N - M \ln(N-2k) = -N \ln N + k \ln k + (N-k) \ln(N-k) - \\ &\quad - M \ln(N-2k) - \frac{1}{2} \ln \frac{N}{2\pi(N-k)k} + \dots \end{aligned}$$

The stationary point of that action obeys $\partial S_0 / \partial k = 0$:

$$\ln k - \ln(N-k) + \frac{2M}{N-2k} + \frac{1}{2k} - \frac{1}{2(N-k)} = 0$$

As expected, $k \rightarrow N-k$ changes the sign of this. We seek for the stationary point with $k < N/2$. We have the transcendent equation (terms $\sim 1/k, 1/N$ are neglected)

$$\ln\left(\frac{N}{k} - 1\right) = \frac{2M/N}{1 - 2k/N}$$

This is generally unsolvable, but if we assume that $M/N \gg 1$ then we get $k/N \ll 1$ and

the asymptotics is

$$-\ln \frac{k}{N} = 2 \frac{M}{N}$$

$$k_0 = N e^{-2M/N}$$

We remind that this happens in the regimes $1 \ll M/N \ll \ln N$. At the same time, to have $k \gg 1$ produces the additional constraint $M/N \ll \frac{1}{2} \ln N$. At this saddle point, $k = k_0$, we have

$$\frac{\partial^2 S_0}{\partial k^2} \approx \frac{1}{k} + \frac{1}{N-k} + \frac{4M}{(N-2k)^2} \approx \frac{1}{k_0} + \frac{4M}{N^2} = \frac{1}{N} \left(e^{2M/N} + \frac{4M}{N} \right) \approx \frac{1}{k_0}$$

where we made use of $M/N \gg 1$. The action itself if

$$\begin{aligned} S_0 &= -N \ln N + k_0 \ln k_0 + (N - k_0) \ln(N - k_0) - M \ln(N - 2k_0) - \frac{1}{2} \ln \frac{N}{2\pi(N - k_0)k_0} \\ &\approx -N \ln N + k_0 \ln k_0 + (N - k_0) \left[\ln N + \ln\left(1 - \frac{k_0}{N}\right) \right] - \\ &\quad - M \left[\ln N + \ln\left(1 - \frac{2k_0}{N}\right) \right] - \frac{1}{2} \ln \frac{1}{2\pi k_0} + \frac{1}{2} \ln\left(1 - \frac{k_0}{N}\right) \end{aligned}$$

If we are interested in the exponent and preexponent, we can only omit terms of the order $o(1)$ in S_0 , for example the very last term in the above. We get

$$S_0 \approx -(M + k_0) \ln N + \left(k_0 + \frac{1}{2}\right) \ln k_0 + (N - k_0) \ln\left(1 - \frac{k_0}{N}\right) - M \ln\left(1 - \frac{2k_0}{N}\right) - \frac{1}{2} \ln \frac{1}{2\pi}$$

However, since our solution for k_0 is itself approximate, we should restrict ourselves to exponential accuracy here and keep only major terms, linear in M

$$\begin{aligned} S_0 &= -M \ln N + O\left(k_0 \frac{M}{N}, k_0 \ln N, k_0, k_0 \ln k_0\right) \\ &= -M \ln N + O(k_0 \ln N) \end{aligned}$$

We now integrate using the Poisson formula:

$$\begin{aligned} \sum_{k=0}^{N/2} e^{-S_0(k) - 2ki\chi} &= \sum_{p \in \mathbb{Z}} e^{-S_0(k_0) - 2k_0 i(\chi - \pi p)} \int dk e^{-\frac{1}{2k_0}(k - k_0)^2 - 2(k - k_0)i(\chi - \pi p)} \\ &= \sum_{p \in \mathbb{Z}} e^{-S_0(k_0) - 2k_0 i(\chi - \pi p) - 2(\chi - \pi p)^2 k_0} \sqrt{2\pi k_0} \end{aligned}$$

Assuming ϕ_0 is not close to $\pm\pi$ the above is dominated by the term with $p = 0$ because $k_0 \gg$

1. If we are close to π phase difference, there are two main terms, but, to an exponential accuracy the answer is still the same (the only problem that could possibly arise is alternating-sign sums that might appear later when summing over N and give incorrect results due to the approximation we do now. Maybe this can be mended easily by restoring these terms via replicating the result via $\phi_0 \rightarrow \phi_0 + 2\pi p$). In the above, we only integrated near the saddle-point with $k_0 < N/2$, there remains the symmetric saddle at $N - k_0$. This adds the complex conjugate to the result (but first we must restore some prefactors):

$$\begin{aligned} \frac{i^M e^{i\chi N}}{M! 2^N} \sum_{k=0}^N C_k^N (N - 2k)^M e^{-2ki\chi} &= \\ \sqrt{2\pi k_0} \frac{e^{i\chi N + iM\pi/2}}{M! 2^N} \sum_{p \in \mathbb{Z}} e^{-S_0(k_0) - 2k_0 i(\chi - \pi p) - 2(\chi - \pi p)^2 k_0} + c.c. &= \\ = 2 \frac{\sqrt{2\pi k_0}}{M! 2^N} e^{-S_0} \sum_{p \in \mathbb{Z}} \exp[-2(\chi - \pi p)^2 k_0] \cos \left[-2k_0(\chi - \pi p) + \chi N + \frac{M\pi}{2} \right] \end{aligned}$$

The sum can be written in terms of the elliptic theta-function. But thus is not particularly helpful. Instead, we risk omitting all terms except the $p = 0$ -terms. This preserves exponential accuracy, but risks errors in further summation over N , since that summation may be an alternating sign sum susceptible to minor corrections to the terms. We get

$$2 \frac{\sqrt{2\pi k_0}}{M! 2^N} e^{-S_0} \sum_{p \in \mathbb{Z}} \exp[-\chi^2 k_0] \cos \left[\chi(N - 2k_0) + \frac{M\pi}{2} \right]$$

The next step is to sum this over N . Remember that $k_0 = N e^{-2M/N}$ and $S_0 = S_0(M, N, k_0(M, N))$.

We now have

$$\Re \frac{i^M}{M!} \left(\frac{\alpha}{4} \right)^M \sum_N \left(-\frac{T_\lambda}{4} \right)^{N/2} \sqrt{k_0} e^{-S_0 - \chi^2 k_0 + i\chi(N - 2k_0)}$$

where we omitted a few pre-exponential factors. We now replace $N = 2K$ and rewrite:

$$\frac{1}{M!} \left(\frac{\alpha}{4} \right)^M \Re i^M \sum_N \left(-\frac{T_\lambda}{4} \right)^K \sqrt{k_0} e^{-S_0 - \frac{\phi_0^2 k_0}{4} + i\phi_0(K - k_0)}, \quad k_0 = \frac{K}{2} e^{-M/K}$$

We now again have to use the saddle approximation when summing over K . The total action, as a function of K is

$$S(K) = S_0 + \frac{\phi_0^2 k_0}{4} - i\phi_0(K - k_0) - K \left(\frac{i\pi}{2} + \ln \frac{T_\lambda}{4} \right).$$

We are again looking for the stationary point. At this point we calculate $\partial S / \partial K$ to the main

order. In particular, since we expect $M \gg K$ we may neglect the k_0 -terms that are seen explicitly: we have

$$\begin{aligned}\frac{\partial S}{\partial K} &\simeq \frac{\partial S_0}{\partial K} + i \left(\phi_0 + \frac{\pi}{2} + \ln \frac{T_\lambda}{4} \right) \\ &\simeq -\frac{M}{K} - \left(i\phi_0 + i\frac{\pi}{2} + \ln \frac{T_\lambda}{4} \right)\end{aligned}$$

which immediately gives $K = M/n_\lambda$ where $n_\lambda = \ln(4/T_\lambda)$. This is the same size as before, which is a good sign! Thus, we mainly have to calculate

The projected answer is:

$$\begin{aligned}I &= e^{-Ms} \\ s &= \ln \frac{2}{\alpha} + \int_0^1 \ln n_\lambda d\lambda + o(1)\end{aligned}$$

Single-photon case. Here we simply have one photon with $N = M$ which produces the $(\alpha/4)^M/M!$ factor and therefore, to exponential accuracy we get

$$P \sim T \exp \left[-M \left(2 \ln \frac{4}{\alpha} - \ln M + 1 \right) \right]$$

4.4 Results

Here we collect results for the ionization rate (i.e. probability $P \propto I_M^2$) within exponential accuracy. There are for parametric regimes (for now we forget about the adiabaticity condition – we will later discuss it). We have the notations $M = g_L/\omega$ is the total number of energy quanta needed to ionize. We have $n_* = \ln \frac{1}{T} - \mathbf{twice}$ the optimal size of a photon (in quanta of ω). The amount of photons in a configuration is called N , its optimum amount is $N_* = 2M/n_*$. The results are as follows:

Ionization rate

1. Single-photon case: $M < n_*$. In this case, the tunneling parameter T is so small that it is best to use a single photon to minimize the $T^{N/2}$ factor in the amplitude I_{NM} . Then we have

$$P_1 \sim T \exp \left[-M \left(2 \ln \frac{4}{\alpha} - 2 \ln M + 2 \right) \right] \quad (4.33)$$

2. Fixed number of photons case: $n_* \ll M \ll n_*^2$. In this case it is optimal to use multiple photons, more sepcifically exactly N_* photons (rounded to the nearest integer, of course).

Processes with different N do not contribute (their contribution is negligible). We get

$$P_{N_*} \sim \exp \left[-M \left(2 \ln \frac{2}{\alpha} + 2 \ln n_* + \pi - 2 + \left\{ \frac{M}{n_*} \right\}^2 \frac{n_*^2}{M^2} + O \left(\frac{n_*^3}{M^3} \right) \right) \right] \quad (4.34)$$

Here $\{M/n_*\} \in (-0.5, 0.5)$ stand for the fractional part of the argument (or rather distance to nearest integer). We see that integer effects are important in this regime.

3. Fluctuating photon number case: $n_*^2 \ll M$. Now, for combinatorial reasons, contributions from $N \neq N_*$ become important, and we get

$$P_{N_*+\delta N} \sim \exp \left[-M \left(2 \ln \frac{2}{\alpha} + 2 \ln n_* + \pi - 2 + o(1) \right) \right] \quad (4.35)$$

In this case N fluctuates significantly ($\delta N = N - N_*$ is typically much larger than unity but much smaller than N_* . It can be found if needed). Thus, no integer effects remain.

4. Sub-case of (3) where only Andreev reflection happens: $n_*^2 \ll M \ll n_* e^{n_*}$. In this case we take only left term in each cosine, or only right – this produces the largest contribution to ionization. [At higher M some normal reflections start to happen (combinatorically they become important. Or, in other words, their phase space becomes large – there are many such “trajectories”). This case is very technically involved]. So, if only MAR (multiple Andreev reflection) happens, then we can further refine the expression for the ionization rate and get

$$P_{N_*+\delta N}^{(MAR)} \sim \exp \left[-M \left(2 \ln \frac{2}{\alpha} + 2 \ln n_* + \pi - 2 + \frac{(\pi - |\varphi_0|)^2}{n_*^2} + O \left(\frac{1}{n_*^3} \right) \right) \right] \quad (4.36)$$

Note on all cases and energy dependence: the Green’s function energy depends on the current energy (i.e. sum of energies of all previously absorbed photons). Therefore, T becomes a function of $\lambda = E/g_L$. Note that this dependence is slow – T is rescaled by the very nice function $c(\lambda) = (1 - \sqrt{1 - \lambda^2})/\lambda^2 \in (1/2, 1)$. So that n_* only changes by $-\ln c(0) = \ln 2 \simeq 0.3$. This energy dependence is actually accounted for and is the origin of the $\pi - 2$ terms in expressions for P .

Chapter 5

Discussion

In this chapter the obtained results are summarized and the potential experimental realization of the system is discussed.

5.0.1 Results summary

The results, obtained in chapters 3 and 4 has different potential for experiment realization. The subgap spectra can be obtained through the conductance measurements like was done in [22] and [24]. However as the conductance peak can be weakened by thermal broadening and scattering on the impurities, so it can be difficult to test that there are no states except for Majoranas – especially for the states near the gap. The results of chapter 3 tell, that measuring the system's supercurrent wouldn't be much different from the short Josephson junction problem.

However the ionization rates from the chapter 4 has a potential for being used in experiment. Indeed, if the system has no Majorana state, the ionization rate will at least get a factor of 2 in the exponent, as when there is no Majorana near the barrier, to ionized the the system needs to break a cooper pair from the condensate, thus it needs to overcome the gap twice.

5.0.2 Possible experimental realization

The system, described in chapter 2, can be potentially be built in experimental setup close to the ones used in [22] and [24].

The first problem, that seemingly makes all the work useless, is the fact that !D superconductors don't exists due to the presence of fluctuations. However there is a bypass — one can make superconducting wires artificially, taking a metallic or semiconducting wire and proximiting it to a strong superconductor. This is a well known method, used, for example, in [22] and [24].

The proposed setup, for the system is presented on 5.1. A metallic or semiconducting wire (yellow) is being put on a insulator (gray) and proximitized to couple of superconductors (violet and cyan). It's important to make the superconductors separate, to obtain a phase difference and avoid shortcutting the barrier. The barrier it'self can be created using a gate (red) with a big negative voltage on it. The chemical potentials in the wires can be adjusted in a similar way, by using a gates near each wire (green).

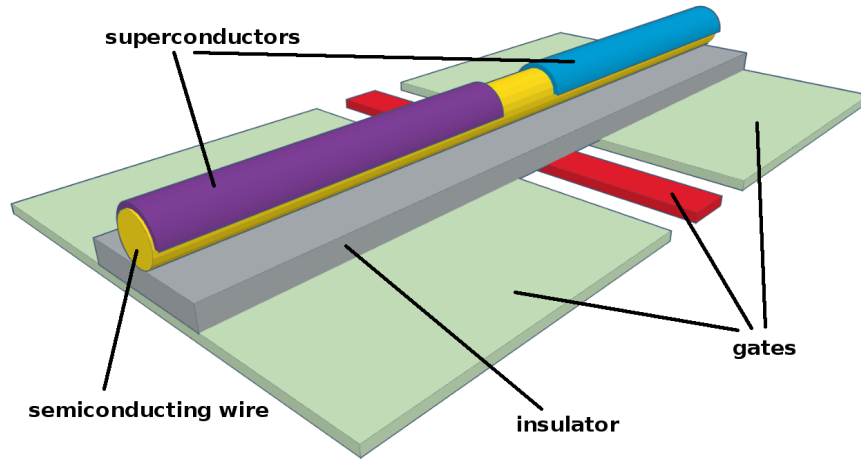


Figure 5.1: Possible experimental realization of the system

The procedure of adjusting the parameters of the model from the chapter 2 can be the following: at first the system is created, with superconductivity inside the wires being as similar, as possible. This may require a really advanced technique of fabricating the samples. After that the magnetic field B turns and adjusts to be a little bigger than Δ . After that the gates should be set to switch the wires to desired topology and create a tunnel barrier.

When the model was chosen it was considered that it's much easier to make spatially inhomogeneous electric than magnetic field. It's also important, that the spin-orbit coupling energy inside the wire should be much stronger than the the superconducting gap. However, this condition can be satisfied as the proximitized superconductivity can be weakened by a proper fabrication process.

Chapter 6

Conclusion

In this work the system of two superconducting wires connected with a tunnel junction is considered. The spectrum is obtained, the supercurrent and the ionization rate for $g_R \gg |g_L|$ is calculated. Despite the fact, that the ionization in this limit is factorized, it possesses its own rich physics with four different regimes of ionization.

Authors hope, that the results of this work can be used for improving the techniques of detecting Majorana fermions in superconducting wires

Appendix A

Wavefunctions for the stationary contact

Here the eigenstates of the junction are presented in leading and subleading order of the tunneling constant t . They are obtained with the methods from the chapter 3 and written in the notation from the section 4.2. Only low and medium momenta parts are presented here, as it's sufficient for the section 4.2, which uses the formulas for from this appendix. The states are normalized as:

$$\langle \gamma_0 | \gamma_0 \rangle = 1 \quad \langle \epsilon, R_0 | \epsilon, R_0 \rangle = N_R(\epsilon) \delta(\epsilon - \epsilon) \quad \langle \epsilon, L_0 | \epsilon, L_0 \rangle = N_L(\epsilon) \delta(\epsilon - \epsilon) \quad (\text{A.1})$$

where

$$N_L(\epsilon) = \frac{4\pi u \sqrt{\epsilon^2 - g_L^2} (e^{2\kappa_L(\epsilon)} + 1)^2}{\epsilon} \quad N_R(\epsilon) = \frac{4\pi u \sqrt{\epsilon^2 - g_R^2} (e^{2\eta_R(\epsilon)} + 1)^2}{\epsilon} \quad (\text{A.2})$$

The definition of the $\eta_{L,R}$, η_L and κ_R is given in the 3.6. The indexes L, R near the spinors are relate to the wire, where this spinor is present. This reference can be used either in $|g_L| < g_R$ or in $|g_L| > g_R$ cases.

The Majorana state is:

$$\langle x | \gamma_0 \rangle = \frac{1}{2} \sqrt{\frac{g_R}{u}} \begin{pmatrix} -1 \\ i \\ -i \\ 1 \end{pmatrix}_R e^{-\frac{g_R x}{u}} \quad (\text{A.3})$$

$$\langle x | \gamma_1 \rangle = \frac{1}{2} \sqrt{\frac{g_R}{u}} \zeta t \left(e^{i\frac{\phi}{2}} + e^{-i\frac{\phi}{2}} \right) \left[\begin{pmatrix} -i \\ 1 \\ 1 \\ -i \end{pmatrix}_L e^{-\frac{2\Delta x}{u}} - i\zeta \begin{pmatrix} -i \\ -1 \\ 1 \\ i \end{pmatrix}_L e^{-\frac{|g_L|x}{u}} \right] \quad (\text{A.4})$$

Continuous states from the right wire are:

$$\langle x|E, R_0\rangle =$$

$$(-ie^{\eta_R(E)} - 1) \begin{pmatrix} -1 \\ -e^{\eta_R(E)} \\ e^{\eta_R(E)} \\ 1 \end{pmatrix}_R e^{-\frac{ix\sqrt{E^2-g_R^2}}{u}} + (e^{\eta_R(E)} + i) \begin{pmatrix} -e^{\eta_R(E)} \\ -1 \\ 1 \\ e^{\eta_R(E)} \end{pmatrix}_R e^{\frac{ix\sqrt{E^2-g_R^2}}{u}} \quad (\text{A.5})$$

$$\langle x|E R_1\rangle \Big|_{E < g_L} = t\zeta (e^{2\eta_R(E)} - 1) \left(e^{i\frac{\phi}{2}} + e^{-i\frac{\phi}{2}} \right) \times$$

$$\times \left[\begin{pmatrix} -i \\ 1 \\ 1 \\ -i \end{pmatrix}_L - e^{-\frac{2\Delta x}{u}} - \frac{2i\zeta}{(1 + e^{-i\theta_L(E)})} \begin{pmatrix} -ie^{-i\theta_L(E)} \\ -1 \\ 1 \\ ie^{-i\theta_L(E)} \end{pmatrix}_L e^{\frac{-x\sqrt{g_L^2-E^2}}{u}} \right] \quad (\text{A.6})$$

$$\langle x|E R_1\rangle \Big|_{E > g_L} = t\zeta (e^{2\eta_R(E)} - 1) \left(e^{i\frac{\phi}{2}} + e^{-i\frac{\phi}{2}} \right) \times$$

$$\times \left[\begin{pmatrix} -i \\ 1 \\ 1 \\ -i \end{pmatrix}_L e^{-\frac{2\Delta x}{u}} - \frac{2i\zeta}{(1 + ie^{-\kappa_L(E)})} \begin{pmatrix} e^{-\kappa_L(E)} \\ -1 \\ 1 \\ -e^{-\kappa_L(E)} \end{pmatrix}_L e^{\frac{ix\sqrt{E^2-g_L^2}}{u}} \right] \quad (\text{A.7})$$

Continuous states from the left wire are:

$$\langle x|\varepsilon, L_0\rangle =$$

$$(e^{\kappa_L(\varepsilon)} - i) \begin{pmatrix} 1 \\ -e^{\kappa_L(\varepsilon)} \\ e^{\kappa_L(\varepsilon)} \\ -1 \end{pmatrix}_L e^{+i\frac{\sqrt{\varepsilon^2-g_L^2}}{u}x} + (-1 + ie^{\kappa_L(\varepsilon)}) \begin{pmatrix} e^{\kappa_L(\varepsilon)} \\ -1 \\ 1 \\ -e^{\kappa_L(\varepsilon)} \end{pmatrix}_L e^{-i\frac{\sqrt{\varepsilon^2-g_L^2}}{u}x} \quad (\text{A.8})$$

$$\begin{aligned}
\langle x|\varepsilon, L_1 \rangle \Big|_{\varepsilon < g_R} &= \zeta t \left(e^{2\kappa_L(\varepsilon)} - 1 \right) \left(e^{i\frac{\phi}{2}} + e^{-i\frac{\phi}{2}} \right) \times \\
&\times \left[\frac{2i\zeta}{(-1 + e^{i\theta_R(\varepsilon)})} \begin{pmatrix} -1 \\ ie^{i\theta_R(\varepsilon)} \\ -ie^{i\theta_R(\varepsilon)} \\ 1 \end{pmatrix}_R e^{-x\frac{\sqrt{g_R^2 - \varepsilon^2}}{u}} + \begin{pmatrix} 1 \\ -i \\ -i \\ 1 \end{pmatrix}_R e^{-\frac{2\Delta x}{u}} \right] \quad (\text{A.9})
\end{aligned}$$

$$\begin{aligned}
\langle x|\varepsilon, L_1 \rangle \Big|_{\varepsilon > g_R} &= \zeta t \left(e^{2\kappa_L(\varepsilon)} - 1 \right) \left(e^{i\frac{\phi}{2}} + e^{-i\frac{\phi}{2}} \right) \times \\
&\times \left[\frac{2it\zeta}{(-1 + ie^{-\eta_R(\varepsilon)})} \begin{pmatrix} -1 \\ -e^{-\eta_R(\varepsilon)} \\ e^{-\eta_R(\varepsilon)} \\ 1 \end{pmatrix}_R e^{\frac{ix\sqrt{E^2 - g_R^2}}{u}} + \begin{pmatrix} 1 \\ -i \\ -i \\ 1 \end{pmatrix}_R e^{-\frac{2\Delta x}{u}} \right] \quad (\text{A.10})
\end{aligned}$$

Appendix B

Multiphoton ionization

This appendix is focused on high-order perturbation theory, ionization rates in particular.

B.1 Basics about Green's functions

The starting point is the general setup of a discrete bound state subject to a weak and slow perturbation $V(t)$. The bound state energy is zero. The goal is to obtain the ionization rate. The time evolution of the wave function obeys the Schroedinger equation:

$$i \frac{\partial}{\partial t} \Psi = (H_0 + V) \Psi \quad (\text{B.1})$$

In the absence of perturbations, the solution is $\Psi(t) = \Psi_0$ (since $E_0 = 0$ it is literally time-independent). For further analysis it's convenient to consider the unperturbed retarded Green's function $G^R(E)$ defined so that:

$$G^R(E)(E + i0 - H_0) = 1 \quad (\text{B.2})$$

If the bound state is normalized, $\langle \gamma | \gamma \rangle = 1$ and the continuous spectrum is normalized according to $\langle E | E' \rangle = N(E) \delta(E - E')$ with some reasonably nice $N(E)$ then:

$$\mathbb{I} = |\gamma\rangle\langle\gamma| + \int \frac{|E\rangle\langle E|}{N(E)} dE \quad (\text{B.3})$$

Similarly, H_0 and G^R in the energy representation:

$$H_0 = \int \frac{|E\rangle\langle E|}{N(E)} E dE \quad G^R(\epsilon) = \frac{|\gamma\rangle\langle\gamma|}{\epsilon + i0} + \int \frac{|E\rangle\langle E|}{(\epsilon + i0 - E)N(E)} dE \quad (\text{B.4})$$

Integrals over E include all states in the continuous spectrum. Where the latter is degenerate, a summation over the degenerate states must be carried out. From now on the "R" index for retarded Green's function will be omitted.

In time representation the Green's function obeys:

$$\left(i\frac{\partial}{\partial t_2} - H_0\right) G(t_2, t_1) = \delta(t_2 - t_1) \quad (\text{B.5})$$

One can formally introduce the Green's function in energy representation with two arguments as a Fourier-transform of $G(t_2, t_1)$:

$$G(E_2, E_1) = \iint e^{iE_2 t_2 - iE_1 t_1} G(t_2, t_1) dt_1 dt_2 \quad (\text{B.6})$$

As H_0 is time independent, $G(t_2, t_1) = G(t_2 - t_1, 0)$, so:

$$G(E_2, E_1) = 2\pi\delta(E_2 - E_1) G(E_1) \quad (\text{B.7})$$

One can also find, that for any eigenstate $|E_0\rangle$

$$G(t) |E_0\rangle = -ie^{-iE_0 t} \theta_H(t) |E_0\rangle \quad (\text{B.8})$$

With the help of Green's function the Schroedinger equation (B.1) can be solved as:

$$\begin{aligned} \Psi(t) = \Psi_0 + \int G_0(t - t') V(t') \Psi_0(t') dt' + \\ \iint G_0(t - t') V(t') G_0(t' - t'') V(t'') \Psi_0(t'') dt' dt'' + \dots \end{aligned} \quad (\text{B.9})$$

where the Ψ_0 is unperturbed wavefunction. This equation can be rewritten by the introduction

B.2 Fermi Golden Rule (first order)

Consider first the lowest order to the Fermi Golden rule by only keeping the linear term in V . Let the Fourier decomposition of V be:

$$V(t) = \sum_n V_n e^{-i\omega_n t} \quad (\text{B.10})$$

(Hermiticity demands $V(t) = V(t)^*$ so that $V_n = V_n^*$). Suppose there is an unperturbed continuous spectrum parameterized by E , with $\langle E | E' \rangle = f(E) \delta(E - E')$. The first step is to calculate

$\langle E|\Psi(t)\rangle$, i.e. the quantum amplitude of being in state $|E\rangle$ at time t . It is:

$$\begin{aligned}
\langle E|\Psi(t)\rangle &= \langle E|\int G_0(t-t')V(t')\Psi_0(t')dt'\rangle = \int \langle E|G_0(t-t')V(t')|\Psi_0\rangle dt' = \\
&= \int \int \langle E|G_0(t-t')|E'\rangle \langle E'|V(t')|\Psi_0\rangle dt' \frac{dE'}{N(E)} \\
&= \int e^{-i(t-t')E} \theta_H(t-t') \langle E|V(t')|\Psi_0\rangle dt' = \\
&= e^{-iEt} \sum_n \int e^{it'(E-\omega_n)} \theta_H(t-t') \langle E|V_n|\Psi_0\rangle dt' \quad (\text{B.11})
\end{aligned}$$

Assuming that the perturbation was turned on at $t' = 0$ the integral over t' is taken from t_0 to t and gives:

$$\langle E|\Psi(t)\rangle = e^{-iEt} \sum_n \langle E|V_n|\Psi_0\rangle \frac{e^{it(E-\omega_n)} - 1}{i(E-\omega_n)} \quad (\text{B.12})$$

Thus, the probability density of being in the state $|E\rangle$ is (omit all frequencies except the resonant one should be omitted since the contributions from non-resonant frequencies can be neglected at long times):

$$\rho(E) = |\langle E|V_n|\Psi_0\rangle|^2 \frac{4 \sin^2 \frac{t(E-\omega_n)}{2}}{(E-\omega_n)^2} \quad (\text{B.13})$$

so that the probability of being in a state between E and $E + \delta E$ is at large times:

$$\begin{aligned}
P(E + \delta E, E) &= |\langle E|V_n|\Psi_0\rangle|^2 \int_E^{E+\delta E} \frac{dE}{N(E)} \frac{4 \sin^2 \frac{t(E-\omega_n)}{2}}{(E-\omega_n)^2} = \\
&= 2t |\langle E|V_n|\Psi_0\rangle|^2 \int_E^{E+\delta E} \frac{d(tE/2)}{N(E)} \frac{4 \sin^2 \frac{t(E-\omega_n)}{2}}{t^2 (E-\omega_n)^2} = \\
&= 2t |\langle E|V_n|\Psi_0\rangle|^2 \frac{\pi}{N(E)} \theta_H(\omega_n - E) \theta_H(E + \delta E - \omega_n) \quad (\text{B.14})
\end{aligned}$$

In other words, the probability density at large t behaves exactly like the δ -function:

$$\rho(E) = 2\pi |\langle E|V_n|\Psi_0\rangle|^2 \delta(E - \omega_n) \quad (\text{B.15})$$

which is the well-known Fermi Golden rule. (Note, that the probability is $dP = \rho(E)dE/f(E)$ – do not forget the normalization). Thus, the ionization rate (i.e. P/t) for a single photon is expressed

as:

$$\mathcal{I} = \frac{2\pi |\langle E | V_n | \Psi_0 \rangle|^2}{f(E)} \quad (\text{B.16})$$

B.3 Fermi Golden Rule (high order)

To treat the higher-order perturbation theory it's convenient to rewrite (B.9) as:

$$\Psi(t) = \Psi_0 + \int \int G_0(t - t') W(t', t'') \Psi_0(t'') dt' dt'' \quad (\text{B.17})$$

where W incorporates all powers of perturbation theory:

$$W = V + V G_0 V + V G_0 V G_0 V + \dots \quad (\text{B.18})$$

The perturbation V in energy space is:

$$\begin{aligned} V(E', E) &\equiv \int V(t', t) e^{it'E' - iEt} dt' dt = \int V(t) e^{i(E' - E)t} dt = \\ &= \sum_n V_n \int e^{i(E' - E - \omega_n)t} dt = \sum_n V_n 2\pi \delta(E' - E - \omega_n) \end{aligned} \quad (\text{B.19})$$

The second term of the perturbation theory $W_2 = V G V$ in energy representation reads:

$$\begin{aligned} W_2(E_2, E_1) &= \int V(E_2, E) G_0(E, E') V(E', E_1) \frac{dE dE'}{(2\pi)^2} = \\ &= \sum_{nm} 2\pi \delta(E_2 - E_1 - \omega_n - \omega_m) V_n G_0(E_1 + \omega_m) V_m \end{aligned} \quad (\text{B.20})$$

Very similarly, the N -th-order term is:

$$W_N(E_2, E_1) = \sum_{n_1, \dots, n_N} 2\pi \delta\left(E_2 - E_1 - \sum_{i=1}^N \omega_{n_i}\right) V_{n_N} \prod_{j=1}^{N-1} G_0\left(E_1 + \sum_{s=1}^j \omega_{n_s}\right) V_{n_j} \quad (\text{B.21})$$

The above expression sums over all processes involving N photons. Note how the Green's functions contains the cumulative energy of all photons absorbed by the time. The δ -function at the start of the expression indicates that the energy is changed by $\sum \omega_{n_i}$. It makes more sense to sort processes within W not by photon count N but rather by the total energy gained, since the total ionization rate should be dominated by ionization to the lowest accessible continuum state.

Defining this activation energy as \mathcal{E} , write:

$$W_{\mathcal{E}}(E_2, E_1) = 2\pi\delta(E_2 - E_1 - \mathcal{E})w_{\mathcal{E}}(E_1) \quad (\text{B.22})$$

$$w_{\mathcal{E}}(E) = \sum_{\{n_i\}:\mathcal{E}} V_{n_N} \prod_{j=1}^{N-1} G_0 \left(E + \sum_{s=1}^j \omega_{n_s} \right) V_{n_j} \quad (\text{B.23})$$

The summation is over all sets of photons n_i that total an energy of \mathcal{E} , i.e. such sets that $\sum_i^N \omega_{n_i} = \mathcal{E}$. The photon number N itself depends on the particular photon set n_i . The total composite perturbation W can be written as a sum of $W_{\mathcal{E}}$ with different \mathcal{E} . However, only one term is relevant — the one with $\mathcal{E} = \min |g_L|, |g_L|$. (If the elementary frequency quantum ω is large enough, this is replaced by the lowest \mathcal{E} that surpasses the minimum gap).

Now the Fermi Golden rule result (B.16) can be rederived for $W_{\mathcal{E}}$. It's easy to see that W has the same energy structure as the single-photon perturbation V . Both operators simply shift the energy. Thus, one may simply put $W_{\mathcal{E}}$ into the Fermi Golden rule instead of V to get the full-theory results:

$$\mathcal{I} = \frac{2\pi |\langle \mathcal{E} | w_{\mathcal{E}} | \Psi_0 \rangle|^2}{N(\mathcal{E})} \quad (\text{B.24})$$

Thus to find the ionization rate one should calculate $w_{\mathcal{E}}$ from (B.23).

Bibliography

- ¹E. Majorana, “Teoria simmetrica dell’elettrone e del positrone”, Il Nuovo Cimento (1937).
- ²S. R. E. Frank T. Avignone and and J. Engel, “Double beta decay, majorana neutrinos, and neutrino mass”, Rev. Mod. Phys. **80**.
- ³A. Giuliani and A. Poves, “Neutrinoless double-beta decay”, Advances in High Energy Physics **2012**.
- ⁴S. Dell’Oro, S. Marcocci, M. Viel, and F. Vissani, “Neutrinoless double beta decay: 2015 review”, Advances in High Energy Physics **27** (2016).
- ⁵R. Jackiw and P. Rossi, “Zero modes of the vortex-fermion system”, Nuclear Physics B **190** (1981).
- ⁶A. Y. Kitaev, “Unpaired majorana fermions in quantum wires”, Uspekhi Fizicheskikh Nauk **44** (2001).
- ⁷N. B. Kopnin and M. M. Salomaa, “Mutual friction in superfluid \mathcal{H}^3 : effects of bound states in the vortex core”, Phys. Rev. B **44** (1991).
- ⁸O. Motrunich, K. Damle, and D. A. Huse, “Griffiths effects and quantum critical points in dirty superconductors without spin-rotation invariance: one-dimensional examples”, Phys. Rev. B **63** (2001).
- ⁹S. D. Sarma, C. Nayak, and S. Tewari, “Proposal to stabilize and detect half-quantum vortices in strontium ruthenate thin films: Non-Abelian braiding statistics of vortices in a $p_x + ip_y$ superconductor”, Phys. Rev. B **73** (2006).
- ¹⁰N. Read and D. Green, “Paired states of fermions in two dimensions with breaking of parity and time-reversal symmetries and the fractional quantum hall effect”, Phys. Rev. B **61** (2000).
- ¹¹T. Senthil and M. P. A. Fisher, “Quasiparticle localization in superconductors with spin-orbit scattering”, Phys. Rev. B **61** (2000).
- ¹²G. Volovik, “Fermion zero modes on vortices in chiral superconductors”, Pisma Zh. Eksp. Teor. Fiz. **70** (1999).
- ¹³L. Fu and C. L. Kane, “Superconducting proximity effect and majorana fermions at the surface of a topological insulator”, Phys. Rev. Lett. **100** (2008).
- ¹⁴R. Aguado, “Majorana quasiparticles in condensed matter”, La Rivista del Nuovo Cimento **40** (2018).

- ¹⁵C. W. J. Beenakker, “Search for majorana fermions in superconductors”, *Annu. Rev. Con. Mat. Phys.* **4** (2013).
- ¹⁶F. von Oppen, Y. Peng, and F. Pientka, *Topological superconducting phases in one dimension* (2014).
- ¹⁷C. Chamon, R. Jackiw, Y. Nishida, S.-Y. Pi, and L. Santos, “Quantizing majorana fermions in a superconductor”, *Phys. Rev. B* **81** (2010).
- ¹⁸S. R. Elliott and M. Franz, “Colloquium: majorana fermions in nuclear, particle, and solid-state physics”, *Rev. Mod. Phys.* **87** (2015).
- ¹⁹J. Alicea, Y. Oreg, G. Refael, F. von Oppen, and M. P. A. Fisher, “Non-abelian statistics and topological quantum information processing in 1d wire networks”, *Nature Physics* **7** (2011).
- ²⁰C. Nayak, S. H. Simon, M. F. Ady Stern, and S. D. Sarma, “Non-abelian anyons and topological quantum computation”, *Rev. Mod. Phys.* **80** (2008).
- ²¹A. Romito, J. Alicea, G. Refael, and F. von Oppen, “Manipulating majorana fermions using supercurrents”, *Phys. Rev. B* **85** (2012).
- ²²V. Mourik, K. Zuo, S. M. Frolov, S. R. Plissard, E. P.A. M. Bakkers, and L. P. Kouwenhoven, “Signatures of majorana fermions in hybrid superconductor-semiconductor nanowire devices”, *Science* **336** (2012).
- ²³S. Vaitiekėnas, M.-T. Deng, P. Krogstrup, and C. M. Marcus, “Flux-induced majorana modes in full-shell nanowires”, *arXiv:1809.05513* (2018).
- ²⁴H. Zhang, C.-X. Liu, S. Gazibegovic, D. Xu, J. A. Logan, G. Wang, N. van Loo, J. D. S. Bommer, M. W. A. de Moor, D. Car, R. L.M. O. het Veld, P. J. van Veldhoven, S. Koelling, M. A. Verheijen, M. Pendharkar, D. J. Pennachio, B. Shojaei, J. S. Lee, C. J. Palmstrøm, E. P.A. M. Bakkers, S. D. Sarma, and L. P. Kouwenhoven, “Quantized majorana conductance”, *Nature* **556** (2018).
- ²⁵Y. Oreg, G. Refael, and F. von Oppen, “Helical liquids and majorana bound states in quantum wires”, *Phys. Rev. Lett.* **105** (2010).
- ²⁶R. Lutchyn, J. Sau, and D. Sarma, “Majorana fermions and a topological phase transition in semiconductor-superconductor heterostructures”, *Phys. Rev. Lett.* **105** (2010).
- ²⁷C. Beenakker, “Three ”universal” mesoscopic josephson effects”, *Transport Phenomena in Mesoscopic Systems* **109**, 235–253 (2004).
- ²⁸E. Akkermans, A. Auerbach, J. E. Avron, and B. Shapiro, “Relation between persistent currents and the scattering matrix”, *Physical Review Letters* **66**, 76 (1991).